

V393  
.R46

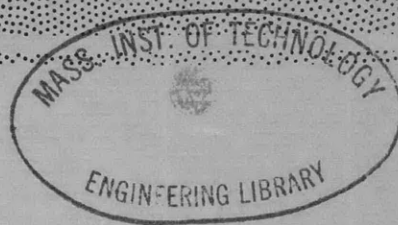
ARIES



3 9080 02753 0242



DEPARTMENT OF THE NAVY



HYDROMECHANICS



AERODYNAMICS



STRUCTURAL  
MECHANICS



APPLIED  
MATHEMATICS

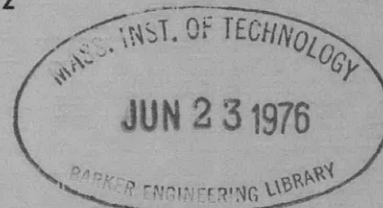


ACOUSTICS AND  
VIBRATION

EXPERIMENTAL DETERMINATION OF STRUCTURAL AND  
STILL WATER DAMPING AND VIRTUAL MASS  
OF CONTROL SURFACES

by

Ralph C. Leibowitz  
and  
Arthur Kilcullen

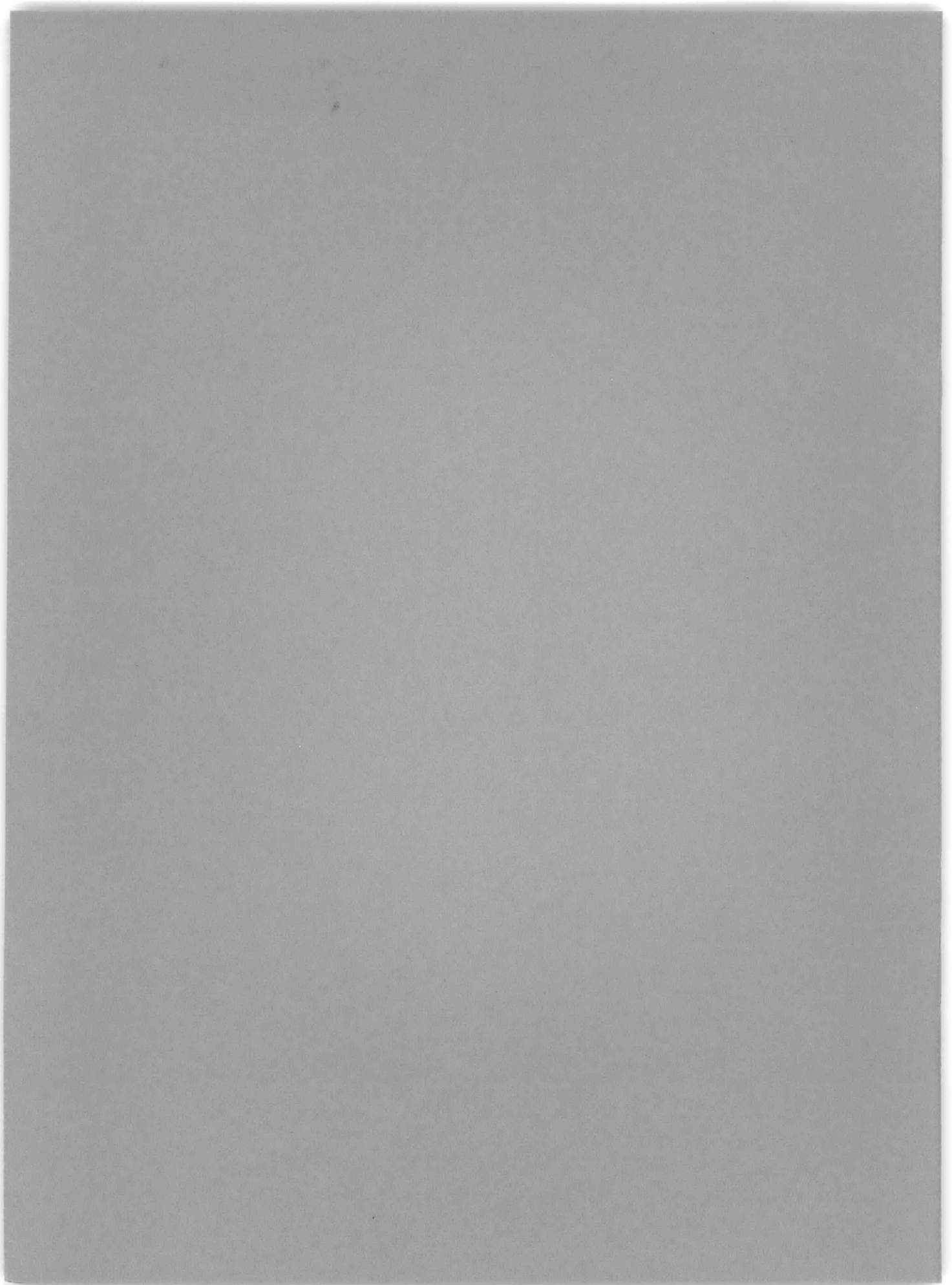


Distribution of this document  
is unlimited.

ACOUSTICS AND VIBRATION LABORATORY  
RESEARCH AND DEVELOPMENT REPORT

April 1965

Report 1836



**EXPERIMENTAL DETERMINATION OF STRUCTURAL AND  
STILL WATER DAMPING AND VIRTUAL MASS  
OF CONTROL SURFACES**

by

**Ralph C. Leibowitz  
and  
Arthur Kilcullen**

**Distribution of this document  
is unlimited.**

**April 1965**

**Report 1836**

## TABLE OF CONTENTS

	Page
Abstract . . . . .	1
Introduction . . . . .	1
Summary of Results . . . . .	2
Description of Rudder-Stock-Hull System . . . . .	2
Theoretical Analysis. . . . .	3
Test Procedure . . . . .	19
Results . . . . .	20
ALBACORE Results . . . . .	27
SAMPSON Results . . . . .	29
Discussion . . . . .	31
Conclusions . . . . .	33
Recommendations . . . . .	34
Acknowledgments . . . . .	34
Appendix A - Development of Equations For Determination of Rudder Motions $\gamma$ , $\alpha$ , $v$ . . . . .	36
Appendix B - Determination of Effective Lengths of Control Surface Stock . . . . .	38
Appendix C - Determination of Logarithmic Decrements . . . . .	48
Appendix D - Derivation of Equations For Parameters C and c . . . . .	51
Appendix E - Determination of Virtual Mass and Mass Moments of Inertia . . . . .	54
References . . . . .	58



## LIST OF FIGURES

	Page
Figure 1 - Location of Gages and Identification of Displacements of Rudder-Stock-Hull System . . . . .	4
Figure 2 - Gage Locations and Orientations for Determining Hull Motions . . . . .	5
Figure 3 - Recording and Analysis Systems . . . . .	20
Figure 4 - Portion of Oscillogram Record (2 channels of 12) from ALBACORE Rudder Vibration Tests . . . . .	27
Figure 5 - Displacements $d_i$ Normalized to Gage 2 for 2 Records from SAMPSON Rudder Vibration Tests . . . . .	30
Figure 6 - Sample of Accelerometer Data Obtained from One Channel of SAMPSON Tests . . . . .	32
Figure 7 - Rudder Coordinates and Location of Gages . . . . .	39
Figure 8 - Curve for Determination of Effective Length of Stock for Bending Motion . . . . .	40
Figure 9 - Curve for Determination of Effective Length of Stock for Rotational Motion (Torsion) . . . . .	42
Figure 10 - Motion of Hull and Rudder, with No Relative Motion between Rudder and Hull . . . . .	44
Figure 11 - Sinusoidal Wave Form Showing Decay due to Viscous Damping . . . . .	49

## LIST OF TABLES

	Page
Table 1 - Summary of Equations of Motion and Parameters	
Associated with Control Surfaces . . . . .	6
Table 2 - Test Results for ALBACORE and SAMPSON . . . . .	21

## NOTATION

A	Amplitude of rotational motion $\alpha$ of the rudder about the x-axis
$A_b$	Amplitude of rotational motion of the hull about the x-axis at the point of attachment of rudder stock to hull (point of attachment here is associated with bending of rudder stock)
b	z-coordinate of effective point of attachment of rudder to rudder stock
C	Damping constant associated with the motion of the rudder in the transverse (y-) direction
$C_c$	Critical damping constant for translational degree of freedom
c	Damping constant associated with the motion of the rudder about the vertical (z-) axis
$c_c$	Critical damping constant for rotational degree of freedom
$d_i$	Displacement of the rudder at the $i^{\text{th}}$ location on the rudder or stock
$d_{R-H}$	Displacement of center of mass of the rudder due to the coupled torsion-horizontal-bending motions of the hull
$(d_{v, \alpha})_{z'}$	Coupled (v, $\alpha$ ) motion of the rudder along the vertical $z'$ -axis through the center of the rudder stock
E	Young's modulus of elasticity
$f_v, f_\gamma, f_{v,a}, f_{v,w}, f_{\gamma,a}, f_{\gamma,w}, f_{\alpha,a}, f_{\alpha,w}$	Frequencies (defined in Appendix E)
G	Shear modulus of elasticity

- g Acceleration of gravity
- h x-coordinate of effective center of attachment of rudder to rudder stock
- I Area moment of inertia of cross section of rudder stock relative to a diameter through the centroid
- $I_p$  Polar moment of inertia of rudder stock about  $z'$ -axis
- $I_z$  Moment of inertia of combined rudder and virtual mass about the z-axis with origin at the effective center of mass of the rudder in water
- $(I_x)_a, (I_z)_a$  Moment of inertia of the rudder about the x- and z-axes respectively with origin at the center of mass of the rudder in air
- $(I_x)_{vir}, (I_z)_{vir}$  Virtual mass moment of inertia of rudder about x- and z-axes respectively with origin at the center of mass of the rudder in water (see Equations [21] and [20] respectively of Table 1 and discussion at end of Appendix E)
- $I_{zx}$  Product of inertia corresponding to  $I_x, I_y, I_z$
- $J_e$  Polar moment of inertia of cross section of rudder stock about a perpendicular axis through the centroid
- $K_1$  Geometrical constants of the rudder (see Appendixes A and B)

$k_s$	Defined as $k_s = \left( \frac{1}{1 + \frac{12EI}{KAG \cdot l^2}} \right) \left( \frac{EI}{l^3} \right)$ where KAG is the shear rigidity of the rudder stock
$L_H, L_P$	Distances between gages on rudder hull system (see Appendix B)
$L_M$	Vertical distance between the $M^{\text{th}}$ gage and Gage 13
$l, l_T$	Effective length of rudder stock from center of gravity of rudder to the points of attachment of rudder stock to hull in bending and torsion, respectively
$m_a$	Mass of the rudder in translation in air
$m_{\text{vir}}$	Virtual mass of the rudder in translation
$m_y$	Total mass of the rudder in translation including virtual mass
$q$	Integer
$S$	Forward speed of ship
$t$	Time
$V$	Amplitude of translational motion ( $v$ ) of the rudder in y-direction
$V_b$	Amplitude of translational motion of the hull in the y-direction at the point of attachment of rudder stock to hull (point of attachment here is associated with bending of rudder stock)
$v$	Small translation of effective center of mass of the rudder in the y-direction
$v_b$	Corresponding translation at the point of attachment of rudder stock to hull

$x, y, z$	Right-handed rectangular coordinates with x-axis always parallel to the ship axis; the origin is always at the effective center of mass of the rudder and the z-axis is vertical and positive upward
$x', y', z'$	As above, but with origin at the point of attachment of rudder to rudder stock
$\bar{x}, \bar{y}, \bar{z}$	Mean chord, height, and thickness of rudder, respectively
$y_p$	Horizontal distance (in y-direction) between Gages 15 and 16
$z'_B$	$z'$ coordinate of point of attachment of stock to hull in bending
$z'_T$	$z'$ coordinate of point of attachment of stock to hull in torsion
$\alpha$	Small rotation of the rudder about x-axis
$\alpha_b$	Small rotation of the hull at the point of attachment of rudder stock to hull about the x-axis (point of attachment here is associated with bending of rudder stock)
$\Gamma$	Amplitude of rotational motion $\gamma$ of the rudder about the z-axis
$\Gamma_b$	Amplitude of rotational motion of the hull about the z-axis at the point of attachment of rudder stock to hull (point of attachment here is associated with torsion of rudder stock)
$\gamma$	Small rotation of the rudder about z-axis
$\gamma_b$	Small rotation of the hull at the point of attachment of rudder stock to hull about the z-axis (point of attachment here is associated with torsion of rudder stock)

$\delta$	Measured values of logarithmic decrements
$\delta_\gamma, \delta_\alpha, \delta_v$	Logarithmic decrements which are defined in Table 1
$\delta_{\gamma R}, \delta_{\alpha R}, \delta_{v R}$	
$\delta_{m(\text{modal})_R}, \delta_{m(\text{modal})_m}$	
$\lambda_i$	Complex circular frequency of vibration of $i^{\text{th}}$ mode
$\mu_i$	Real part of $\lambda_i$ indicating the degree of damping
$\rho$	Density of seawater
$\tau$	Period of oscillation
$\phi_i$	Phase angles defined in Appendix D
$\omega_i$	Imaginary part of $\lambda_i$ indicating circular frequency of oscillation





## ABSTRACT

An experiment has been designed for determining the damping constants and virtual mass for the control surface systems of USS ALBACORE (AGSS 569) and USS SAMPSON (DDG 10); theoretical methods for determining the virtual inertias (including virtual mass) of these control surfaces are also given. The theoretical foundation for the experimental design and the procedure for analyzing the experimental data to obtain the parameters are described. These damping and inertial parameters are essential to the performance of a hull-control surface vibration and/or flutter analysis.<sup>1-5</sup>

## INTRODUCTION

The solution for the vibrations and flutter characteristics of a combined hull-control surface system can be obtained if the physical and hydroelastic parameters in the equations of motion representing the system<sup>1</sup> are evaluated; the theory underlying the derivation of these equations has been shown to have some degree of verification.<sup>3</sup> The method of evaluation of physical (mass-elastic) parameters associated with equations of motion of the hull alone is given in Reference 5. The method of evaluation of certain hydroelastic parameters for the control surface (e. g. , rudder and/or diving plane) is given in Reference 2.

The primary objective of this report is to add to the method of evaluation of the control surface parameters by describing experimentally based methods for computing damping constants and virtual mass for the

---

<sup>1</sup> References are listed on page 58.

control surface. In addition, certain equations are presented for calculating the virtual inertias (including virtual mass) by theory alone. The entire procedure is demonstrated for the case of two ships, USS ALBACORE (A655569) and USS SAMPSON (DDG10).

## SUMMARY OF RESULTS

Equations and other identifying material for the experimental determination of control surface\* and hull motions, the logarithmic decrement and damping for these motions, the virtual mass and virtual mass moments of inertia of the control surface about axes through its center of mass are given in Table 1. These motions are due to an impulsive load acting on the control surface. The equations developed are applicable for motion associated with a single frequency; thus, each modal frequency of a complex motion is treated in turn. Extension to several superposed modes is discussed in the text.

## DESCRIPTION OF RUDDER-STOCK-HULL SYSTEM

The representation of a rudder-stock-hull system\*\* and its motions is based on the following assumptions:

1. The rudder is considered to be a rigid body attached to a flexible

---

\* The control surfaces considered here are rudders and stern planes.

\*\* Stern plane-hull systems are similarly treated.

stock, which, in turn, is attached to a flexible hull. The point of attachment of the rudder to the stock will be different for each rudder system. In this report it will be assumed to be located at the top of the rudder.\*

2. Of the six possible motions of the rudder associated with a symmetrical rigid rudder-flexible stock system, only three contribute significantly to the total coupled athwartship motion. These are the rotations  $\gamma$  and  $\alpha$  about the z- and x-axes and the translation  $v$  along the y-axis respectively (see Figure 1).

3. Small vibration theory is applicable, i. e., the system is linear for small angular and translational displacements.

4. The combined still water and structural damping force is proportional to the velocity of the rudder, i. e., viscous damping is assumed.

#### THEORETICAL ANALYSIS

The analysis underlying the derivation of the equations in Table 1 is described in this section.

Figures 1 and 2 are schematic diagrams of the instrumentation of the rudder-stock-hull system. The  $d_i$ 's in these figures represents the displacements of the system at the points indicated when the rudder-stock-hull system is set into free vibration by an impulsive loading on the rudder. Kinematic relationships between the displacements  $d_i$  and the

---

\* For the ships tested here, the stocks were welded into the control surfaces such that the portion of the stock within the surface moves rigidly with the surface.

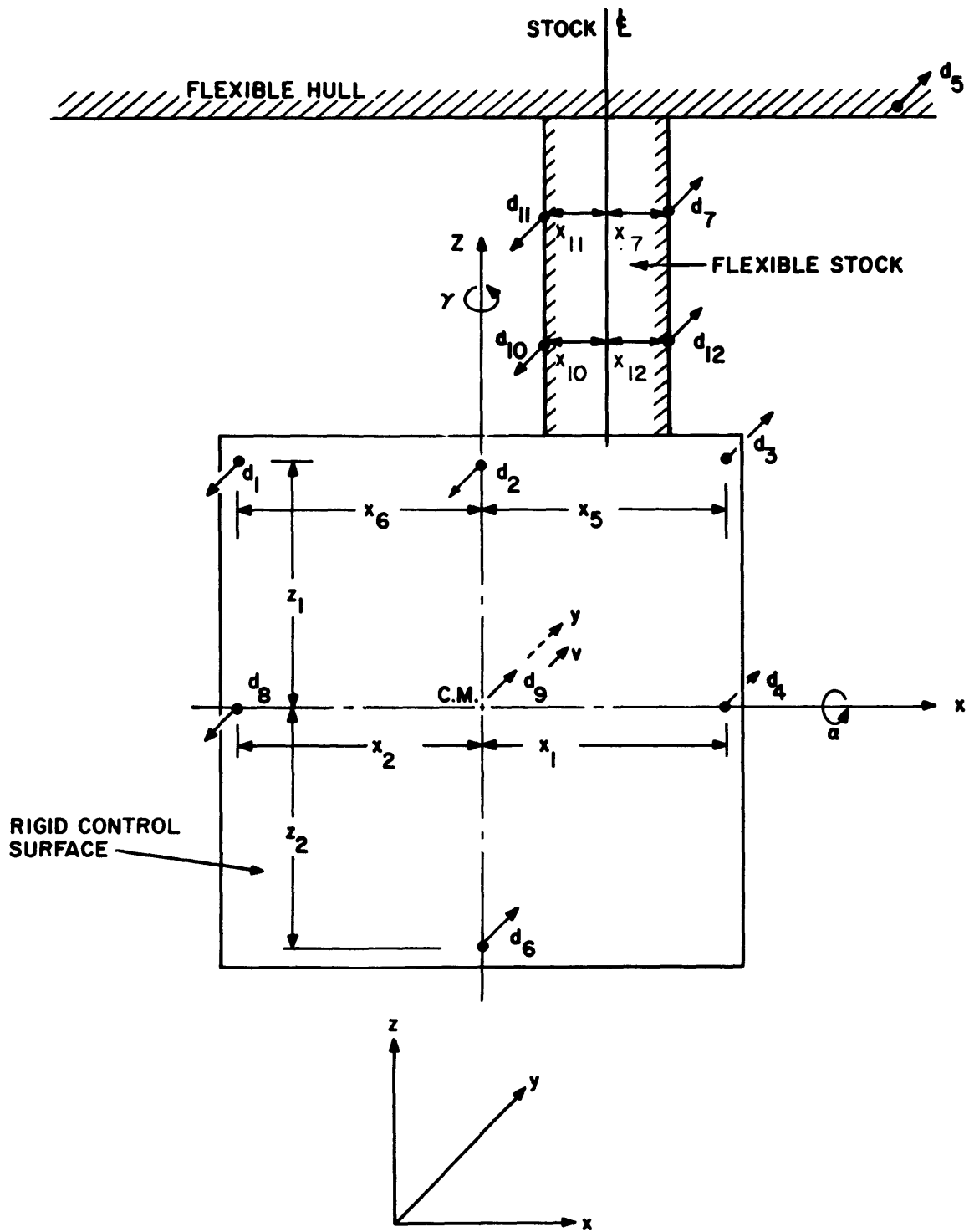


Figure 1. Location of Gages and Identification of Displacements of Rudder-Stock-Hull System.

corresponding components for rotational and translational motions  $\gamma$ ,  $\alpha$ , and  $v$  about the  $z$ - and  $x$ -axes respectively and along the  $y$ -axis, are derived in Appendix A. The resulting equations (1) through (3b) are summarized in Table 1.

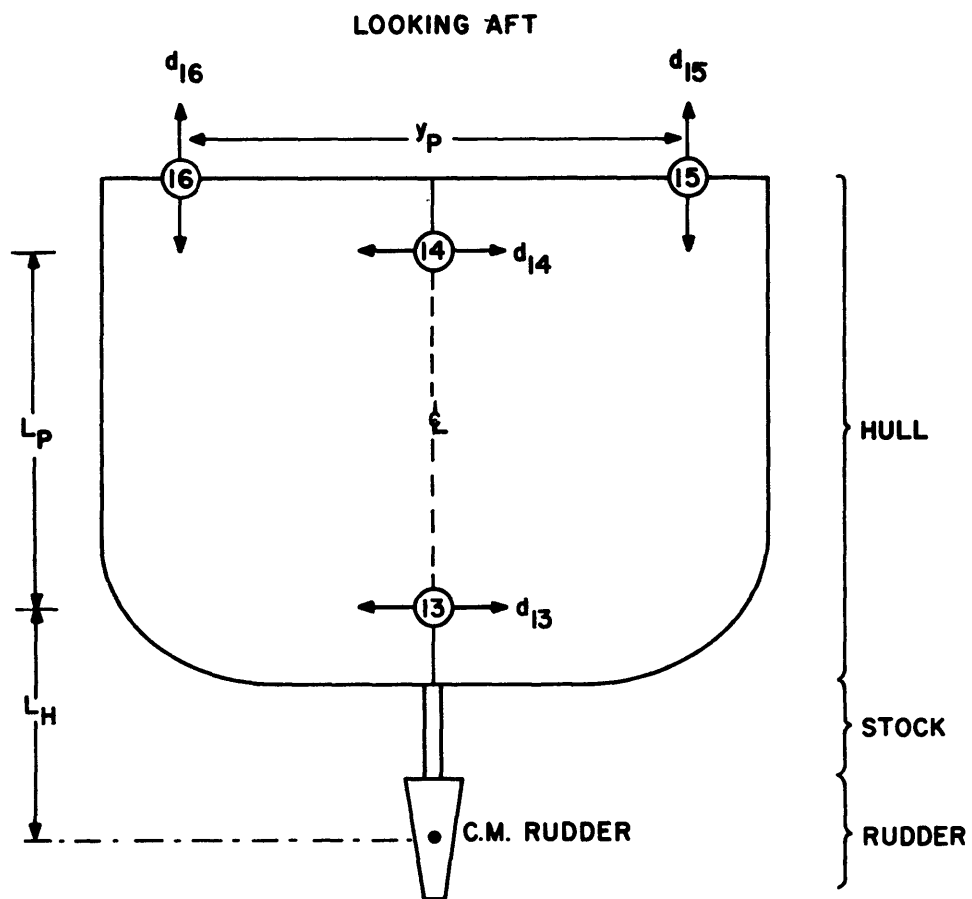


Figure 2. Gage Locations and Orientations for Determining Hull Motions.

TABLE 1

Summary of Equations of Motion and Parameters Associated with Control Surfaces\*

NUMBER	EQUATION	ASSOCIATED CONSTANTS	DEFINITION AND REMARKS	SOURCE
1	$\gamma(t) = K_1(d_4 - d_8)**$	$K_1 = \frac{1}{x_1+x_2} ***$	Total rotational motion of the rudder about the z-axis.	Appendix A
2	$\alpha(t) = K_2(d_6 - d_2)$	$K_2 = \frac{1}{z_1+z_2}$	Total rotational motion of the rudder about the x-axis.	Appendix A
3a	$v(t) = K_3(d_2+K_4d_6)$	$K_3 = \frac{z_2}{z_1+z_2}$ $K_4 = \frac{z_1}{z_2}$	Total translational motion of the rudder along the y-axis.	Appendix A
3b	$v(t) = K_5(d_4+K_6d_8)$	$K_5 = \frac{x_2}{x_1+x_2}$	Total translational motion of the rudder along the y-axis.	Appendix A
4	$\delta_y = \frac{1}{q} \log_e \left[ \frac{(d_4 - d_8)_{t=t_0}}{(d_4 - d_8)_{t=t_0+q\tau}} \right]$	$K_6 = \frac{x_1}{x_2}$ $q = \text{integer}$ $\tau = \text{period of oscillation.}$	Logarithmic decrement of $\gamma(t)$ motion.	Appendix C
5	$\delta_\alpha = \frac{1}{q} \log_e \left[ \frac{(d_6 - d_2)_{t=t_0}}{(d_6 - d_2)_{t=t_0+q\tau}} \right]$		Logarithmic decrement of $\alpha(t)$ motion.	Appendix C



TABLE 1 (CONT'D)

NUMBER	EQUATION	ASSOCIATED CONSTANTS	DEFINITION AND REMARKS	SOURCE
6a	$\delta_v = \frac{1}{q} \log_e \left[ \frac{(d_2 + K_4 d_6)_{t=t_0}}{(d_2 + K_4 d_6)_{t=t_0 + q\tau}} \right]$		Logarithmic decrement of v(t) motion.	Appendix C
6b	$\delta_v = \frac{1}{q} \log_e \left[ \frac{(d_4 + K_6 d_8)_{t=t_0}}{(d_4 + K_6 d_8)_{t=t_0 + q\tau}} \right]$		Logarithmic decrement of v(t) motion.	Appendix C
7	$\delta_{(\text{modal})_M} = \frac{1}{q} \log_e \left[ \frac{(d_M)_{t=t_0}}{(d_M)_{t=t_0 + q\tau}} \right]$		Logarithmic decrement of the total recorded motion at the M <sup>th</sup> position.	Appendix C
8a	$\alpha_b(t) = \frac{d_{13} - d_{14}}{L_P}$	Constants $L_P, y_P$ , defined in Appendix B and Figure 2.	Contribution of the $\alpha(t)$ motion of the hull to the total recorded motion of the control surface.	Appendix B
8b	$\alpha_b(t) = \frac{d_{16} - d_{15}}{y_P}$		Contribution of the $\alpha(t)$ motion of the hull to the total recorded motion of the control surface.	Appendix B

2

TABLE 1 (CONT'D)

NUMBER	EQUATION	ASSOCIATED CONSTANTS	DEFINITION AND REMARKS	SOURCE
9	$d_{R-H}(t) = d_{13} + L_H \alpha_b$	Constant $L_H$ defined in Appendix B and Figure 2.	Displacement of center of mass of the rudder due to the coupled torsion-horizontal-bending motions of the hull. The contribution of $\gamma_b(t)$ to $d_{R-H}(t)$ in the present application has been neglected. See Equation [B-19] and footnote in Appendix C. The more general expression is given by Equation [B-15].	Appendix B
10	$\delta\gamma_R = \frac{1}{q} \log_e \left\{ \frac{[K_1(d_4 - d_8) - \gamma_b]_{t=t_0}}{[K_1(d_4 - d_8) - \gamma_b]_{t=t_0 + q\tau}} \right\}$		Logarithmic decrement of the rotational motion of the rudder relative to the hull about the z-axis. $\gamma_b$ computed in accordance with the procedure of Appendix B.	Appendix C
11	$\delta\alpha_R = \frac{1}{q} \log_e \left\{ \frac{[K_2(d_6 - d_2) - \alpha_b]_{t=t_0}}{[K_2(d_6 - d_2) - \alpha_b]_{t=t_0 + q\tau}} \right\}$		Logarithmic decrement of the rotational motion of the rudder relative to the hull about the x-axis. $\alpha_b$ computed in accordance with the procedure of Appendix B.	Appendix C

∞

TABLE 1 (CONT'D)

NUMBER	EQUATION	ASSOCIATED CONSTANTS	DEFINITION AND REMARKS	SOURCE
12a	$\delta_{v_R} = \frac{1}{q} \log_e \left\{ \frac{[K_3(d_2 + K_4 d_6) - d_{R-H}]_{t=t_0}}{[K_3(d_2 + K_4 d_6) - d_{R-H}]_{t=t_0 + q\tau}} \right\}$		<p>Logarithmic decrement of the translational motion of the rudder relative to the hull along the y-axis.</p>	<p>Appendix C</p>
12b	$\delta_{v_R} = \frac{1}{q} \log_e \left\{ \frac{[K_5(d_4 + K_6 d_8) - d_{R-H}]_{t=t_0}}{[K_5(d_4 + K_6 d_8) - d_{R-H}]_{t=t_0 + q\tau}} \right\}$		<p>Logarithmic decrement of the translational motion of the rudder relative to the hull along the y-axis.</p>	<p>Appendix C</p>
13	$\delta_{M(\text{modal})_R} = \frac{1}{q} \log_e \left\{ \frac{[d_M - (d_{13} + L_M \alpha - X_M \gamma)_b]_{t=t_0}}{[d_M - (d_{13} + L_M \alpha - X_M \gamma)_b]_{t=t_0 + q\tau}} \right\}$	<p>Constants <math>L_M</math>, <math>X_M</math>, defined in Appendixes B and C.</p>	<p>Logarithmic decrement of the relative displacement between rudder and hull at the <math>M^{\text{th}}</math> location. Note that the term <math>X_M \gamma_b</math> was considered negligible in the present application.</p>	<p>Appendixes B and C</p>

TABLE 1 (CONT'D)

NUMBER	EQUATION	ASSOCIATED CONSTANTS	DEFINITION AND REMARKS	SOURCE
14	$C = -2m_y \mu + \frac{12k_s}{v_1 \omega} \left[ v_{b2} - h\gamma_2 + b\alpha_2 - \frac{t}{2} (\alpha_2 + \alpha_{b2}) \right]$	<p>All constants are defined in Appendix B or in Notation.</p>	<p>Damping constant associated with the motion of the rudder along the y-direction.</p>	<p>Appendix D</p>
15	$c = \frac{1}{(\gamma_1 - \gamma_{b1})\omega + (\gamma_2 - \gamma_{b2})\mu} \left\{ \begin{aligned} & -I_z \left[ \gamma_2 (\mu^2 - \omega^2) + 2\gamma_1 \mu \omega \right] \\ & + I_{xz} \left[ \alpha_2 (\mu^2 - \omega^2) + 2\alpha_1 \mu \omega \right] \\ & + 12k_s h \left[ v_{b2} - h\gamma_2 + b\alpha_2 + \frac{t}{2} (\alpha_2 + \alpha_{b2}) - \frac{GJ}{t_T} (\gamma_2 - \gamma_{b2}) \right] \end{aligned} \right\}$	<p>All constants are defined in Appendix B or in Notation.</p>	<p>Damping constant associated with the motion of the rudder about the z-axis.</p>	<p>Appendix D</p>
16	$C = -2m_y \mu = 2m_y f \delta$	$f = \omega / 2\pi$ $-\frac{\mu}{\omega} = \frac{\delta_v}{2\pi}$	<p>Approximated form of Equation [14] where it is assumed that <math>\gamma_2 = \alpha_2 = \alpha_{b2} = v_{b2} = 0</math> (see Discussion).</p>	<p>Appendix D</p>
17	$c = 2 \left( I_{z \ xz} - I_{xz} \frac{\alpha_1}{\gamma_1} \right) f \delta_y$	$-\frac{\mu}{\omega} = \frac{\delta_y}{2\pi}$	<p>Approximated form of Equation [15] where it is assumed that <math>\gamma_2 = \alpha_2 = \gamma_{b1} = \gamma_{b2} = \alpha_{b2} = v_{b2} = 0</math> (see Discussion).</p>	<p>Appendix D</p>

TABLE 1 (CONT'D)

NUMBER	EQUATION	ASSOCIATED CONSTANTS	DEFINITION AND REMARKS	SOURCE
18	$m_{\text{vir}} = m_a \left[ \left( \frac{f_{v,a}}{f_{v,w}} \right)^2 - 1 \right]$		Virtual mass of rudder in translation. All terms defined in Appendix E.	Appendix E
19	$m_{\text{vir}} = \pi \frac{\rho}{g} \left( \frac{\bar{x}}{2} \right)^2 \bar{z}$	$g = 32.17 \text{ ft/sec}^2$ $\rho = 64.15 \text{ lb/ft}^3$ $\bar{x}$ = mean chord of rudder $\bar{z}$ = mean vertical height of rudder	Virtual mass of rudder in translation.	Ref. 15, Ref. 4, Ref. 5 (43)
20	$(I_z)_{\text{vir}} = \frac{\pi \rho}{8 g} \left[ \left( \frac{\bar{x}}{2} \right)^2 - \left( \frac{\bar{y}}{2} \right)^2 \right] \bar{z} + r^2 m_{\text{vir}}$	$\bar{y}$ = mean width of rudder in y-direction; r defined in Appendix E.	Virtual mass moment of inertia of rudder about z-axis with origin as the center of mass of the rudder in water.	Ref. 15, Ref. 4 (Table 4), Appendix E

TABLE 1 (CONT'D)

NUMBER	EQUATION	ASSOCIATED CONSTANTS	DEFINITION AND REMARKS	SOURCE
21	$(I)_{x \text{ vir}} = \frac{3\pi}{20} \frac{\rho}{g} \left( \frac{z}{2} \right)^4 \bar{x} + s^2 m_{\text{vir}}$	s defined in Appendix E.	Virtual mass moment of inertia of rudder about x-axis with origin at the center of mass of the rudder in water.	Ref. 15, Ref. 4 (Table 4), Appendix E
<p>* Values for parameters <math>l</math> and <math>l_T</math>, the effective lengths of stock for bending and torsion, respectively, are computed by extrapolation or interpolation methods given in Appendix B.</p> <p>** <math>d_i = d_i(t)</math></p> <p>*** Constants <math>x_i</math> and <math>z_i</math> are defined in Figure 1.</p>				

The preceding analysis for the rudder vibration includes the contributions of the hull motion for during a vibration of the entire rudder-hull system, the flexible hull also translates and rotates along the y- and about the x- and z-axes, respectively. Hence, the hull's motional contribution must be subtracted from the recorded rudder motions in order to determine the motions of the rudder relative to the hull; this is equivalent to finding the motions of the rudder system (rudder and effective length of stock) attached to a rigid hull. The hull motions are considered to be applied to the rudder stock at the effective points of attachment of rudder stock to hull. These points of attachment for bending and torsion of the rudder stock which permit us to compute corresponding effective lengths of the stock are determined from the recorded data by extrapolation and interpolation methods as explained in Appendix B.

The effects of motions of the tiller and steering system upon the total recorded motion of the rudder have not been included in this analysis. In some problems, these effects may be significant enough to require an extended treatment of the analysis presented here. The methods basic to this extension will be similar to those given in the text; the detailed procedure will depend upon the particular application, i. e., the particular hull-rudder system.



Equations [4] - [6b] of Table 1, which are derived in Appendix C, define the logarithmic decrements of the  $\gamma$ ,  $\alpha$ , and  $v$  motions corresponding to the transient displacements of the rudder system including the contributions of the hull motions.\* Similarly, Equation [7] is the decrement for the coupled  $\gamma$ ,  $\alpha$ ,  $v$  motions.\*\* The corresponding decrements for the motions of the rudder relative to the hull are given by Equations [10] - [12] using Equations [8] and [9] and the procedure given in Appendix B for obtaining  $\gamma_b$ ; see Appendix C. Equation [13], also derived in Appendix C, defines the modal decrement of the rudder motions relative to the hull.

The method for determining the zero speed damping parameters of the rudder and the relationship between these parameters and the logarithmic decrements of the rudder is now treated (see Appendix D).

Page 78 of Reference 1 gives the several damping parameters associated with motions  $\dot{\gamma}$  and  $\dot{\alpha}$  and  $\dot{v}$  of the rudder. Of these several parameters,

---

\* The logarithmic decrement corresponds to a single mode of vibration (i.e., decaying sinusoidal oscillation). Consideration for several superposed modes is discussed in the text. To obtain each decrement, we look at the motion in one degree of freedom at a time, ignoring the motions in the other two degrees of freedom.

\*\* Here the logarithmic decrement is for one mode of vibration of the rudder system including the contributions of the motions  $\alpha$ ,  $\gamma$ , and  $v$  in the three degrees of freedom.

only the parameters  $C$  and  $c$  associated with rudder translation athwartship (along  $y$ -) and rudder rotation about an axis parallel to the stock (about  $z$ -) have been considered as significant and are therefore the only ones included in the equations of motion (62a, b) of Reference 1, which are the basis for determining the damping parameter values here.

Since we are considering the damping of the system in still water, terms containing  $S$  (ship speed) in Equations [62a, b] are equated to zero. Also, since damping in the  $\alpha$  degree of freedom will be assumed to be negligible, Equation [62c] is omitted from the discussion. Equations [62a, b] may be used directly to obtain (at zero speed) the parameters  $C$  and  $c$  in terms of the variables  $\gamma, \alpha, v, \gamma_b, \alpha_b, v_b$  and certain geometrical and physical parameters.

The variables are obtained from the test records and the constants are determined by the methods of Reference 2 and/or from measurements. It may turn out that when variables obtained from one portion of the records are inserted into these equations, the calculated values of  $C$  and  $c$  are different from those corresponding to the variables obtained from another portion of the record. This indicates that  $C=C(t)$  and  $c=c(t)$ . If the variation is small, then  $C$  and  $c$  may be sensibly considered to be constant for convenience. If the record shows that the modes are discrete at different times, then each mode may in turn be treated as predominant over the pertinent time interval and substitution of the variables will show

if  $C$  and  $c$  vary with the mode (or frequency), i. e., whether  $C=C(\omega)$ ,  $c=c(\omega)$ . Appendix D gives the derivation of the resulting Equations [14] and [15] which are based upon Equations [62a, b] of Reference 1. In these equations,  $-\frac{\mu}{\omega} = \frac{\delta}{2\pi} = \frac{C}{C_c} = \frac{c}{c_c}$  (see Reference 3) where  $\delta$  is the logarithmic decrement of the wave form,  $\mu$  is the real part of  $\lambda$  indicating the degree of damping, and  $\omega$  is the imaginary part of  $\lambda$  which is the circular frequency of vibration; i. e.,  $\lambda = \mu + j\omega$ ;  $\delta, \omega$  (and hence  $\mu$ ) are directly obtainable from the wave-form on a given record for a particular mode of vibration.  $C_c$  and  $c_c$  are critical damping constants for the translational and rotational degrees of freedom, respectively.

If all modes, or two of the three modes, persist simultaneously, then each mode may be filtered in turn from a taped signal and an oscillogram of the filtered mode signal can be obtained. Thus postulating that  $v(t)$  may be represented by:

$$v(t) = \sum_{i=1}^3 v_i e^{\lambda_i t}$$

where

$$\lambda_i = \mu_i + j\omega_i \quad i = 1, 2, 3$$

Then if the  $i^{\text{th}}$  mode predominates for a particular period of time or is filtered out of the taped signal, the equation for  $v(t)$  becomes

$$v(t) = v_i e^{\lambda_i t} \quad i = 1, 2, 3$$

for the corresponding signal and similarly for the variables  $\gamma, \alpha, v_b, \gamma_b, \alpha_b$  (see Appendix D).

Equations [62a, b] of Reference 1 may be solved to obtain  $C/C_c$  or  $\frac{c}{c} = -\frac{\mu}{\omega}$  by the analytic procedures of Reference 3.\* This value may be compared with  $C/C_c$  or  $c/c_c = \frac{\delta}{2\pi}$  obtained from the measurements described above and in Appendix C. Close agreement would indicate that the computation for  $C/C_c$  and  $c/c_c$  from experimental data as prescribed here is valid. It should be noted that for a particular mode, the decay ratio for translational motion  $v$  alone is the same as that for rotational motion  $\gamma$  alone or  $\alpha$  alone and is also the same as that for the total displacement (at any point on the rudder) consisting of contributions of the coupled motions  $\gamma, \alpha,$  and  $v$ .

When more than one mode is present simultaneously, each contributes to the  $v$  (or  $\alpha$  or  $\gamma$ ) motion. The motion in each degree of freedom may then be considered to be the sum of sinusoids with frequencies corresponding to the modes present. Note that the phase relationships are also included in the equations.

---

\* Details of the method of solution of the decay ratio  $C/C_c$  and application to actual problems are given in this reference.

Thus in general

$$v(t) = \sum_{i=1}^3 e^{\mu_i t} (v_{i,1} \sin \omega_i t + v_{i,2} \cos \omega_i t)$$

$$v_b(t) = \sum_{i=1}^3 e^{\mu_i t} (v_{i,b1} \sin \omega_i t + v_{i,b2} \cos \omega_i t)$$

$$\alpha(t) = \sum_{i=1}^3 e^{\mu_i t} (\alpha_{i,1} \sin \omega_i t + \alpha_{i,2} \cos \omega_i t)$$

with similar expressions for  $\alpha_b, \gamma, \gamma_b$ . The equations for these variables and their derivatives may then be substituted into Equation [62a, b] and  $C_i$  and  $c_i$  found in a manner similar to that given above for  $i = 1$  or  $2$  or  $3$  only. The resulting equations which are more complex will not be given here but can be easily obtained.

The mass and flexibility of the rudder can be calculated using the methods of References 4 or 5. Extension of the damping computation to include certain damping constants omitted in deriving Equation [62] of Reference 1 can be performed using the methods of Reference 6.

## TEST PROCEDURE

The computation of the parameters  $c$ ,  $C$ ,  $l$ ,  $C/C_c$ , etc. requires that experimental data be obtained for insertion into the equations of Table 1.

This section describes the test procedure for obtaining such data.

Figures 1 and 2 show the schematic diagrams of the rudder, rudder stock, and hull with accelerometers at locations  $d_i$  which are directed normal to the vertical centerplanes of the rudder-stock and hull. Care must be taken to locate (i. e., compute prior to testing) the exact center of mass\* of the rudder in order to accurately determine the rotational and translational components of the total measured motion of the rudder.

The rudder-hull system was set into free vibration by impulsive excitation of the rudder. The excitation was produced by a snub-nosed ram capable of creating an impulsive load of large magnitude with duration sufficient to excite the lower modes of vibration. Excitations are produced at different locations on the rudder in order to agitate all (lower) modes of interest.

The vibratory responses picked up by the accelerometers are converted into electrical signals which are then amplified and recorded onto magnetic tape or oscillograph charts. Figures 3a and 3b are block diagrams of the recording systems used in the ALBACORE and SAMPSON tests, respectively.

In general, such tests are to be performed in air and in water.

---

\*See footnote, page 36 of Appendix A.

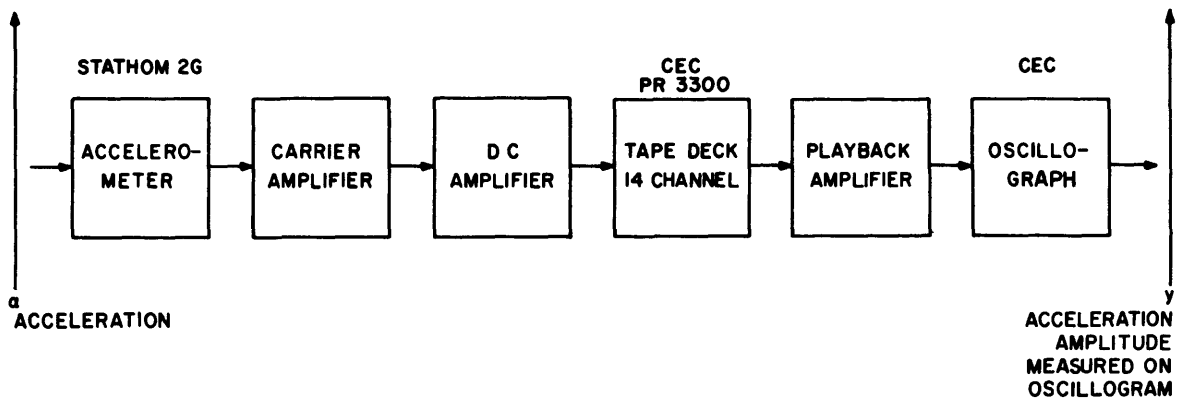


Figure 3a - Recording System for Rudder Vibration Trials of ALBACORE

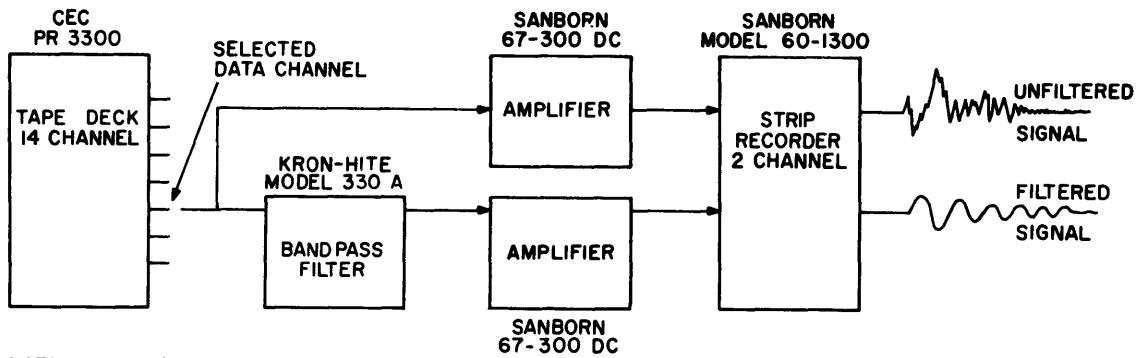


Figure 3b - Data Analysis for Rudder Vibration Trials of SAMPSON

Figure 3. Recording and Analysis Systems.

## RESULTS

The results of analyzing the data obtained from zero speed tests in drydock flooded and unflooded on ALBACORE and SAMPSON are shown in Table 2. The methods of data analysis yielding these results are now discussed.



TABLE 2

Test Results for ALBACORE and SAMPSON

USS ALBACORE (AGSS 569)

1. RUDDER (a)

MEASURED FREQUENCIES (cps)	
In Air	In Water
20.1	13.0 (predominant)
24.5 (predominant)	45
123	80
	87

(b)

LOGARITHMIC DECREMENTS					
In Air (24.5 cps)				In Water (13.0 cps)	
EQUATION NUMBER*	DECREMENT**	VALUE	PERCENT DEVIATION FROM AVERAGE	VALUE	PERCENT DEVIATION FROM AVERAGE
4	$\delta_v$	0.0524	-23.4	0.0952	-20.8
5	$\delta_\alpha$	0.0671	- 2.0	0.0936	-22.3
6a	$\delta_v$	0.0758	+10.8	0.1212	+ 0.1
7	$\delta_{\text{modal}}$	0.0783	+14.5	0.1717	+42.5
AVERAGE		0.0684	±12.1	0.1285	±21.3
*See Table 1                      **See Notation					

TABLE 2 (CONT'D)

(c)

DAMPING CONSTANTS				
EQUATION NUMBER*	In Air (24.5-cps)		In Water (13.0-cps)	
16	C = 0.3261 ton-sec/ft		C = 1.1424 ton-sec/ft	
17	c = 0.1655 ft-ton-sec		c = 1.2346 ft-ton-sec	
	QUANTITY	SOURCE	QUANTITY	SOURCE
	$m_a = 0.0878 \text{ ton-sec}^2/\text{ft}$	Reference 4, Table 4	$m_y = 0.3613 \text{ ton-sec}^2/\text{ft}$	Reference 4, Table 4
	$I_z = 0.3320 \text{ ft-ton-sec}^2$	Ship Plans	$I_z = 0.6446 \text{ ft-ton-sec}^2$	Reference 4, Table 4
	$I_{xz} = -0.1687 \text{ ft-ton-sec}^2$	Ship Plans	$I_{xz} = -0.1514 \text{ ft-ton-sec}^2$	Reference 4, Table 4
DATA**	$\omega = 2\pi \times 24.5 \text{ sec}^{-1}$	Table 2a	$\omega = 2\pi \times 13.0 \text{ sec}^{-1}$	Table 2a
	$\alpha_1/\gamma_1 = -1.5877$	Experimental Data	$\alpha_1/\gamma_1 = -0.9631$	Experimental Data
	$\delta_v = 0.0758$	Table 2b	$\delta_v = 0.1216$	Table 2b
	$\delta_\gamma = 0.0524$	Table 2b	$\delta_\gamma = 0.0952$	Table 2b
*See Table 1      **See Notation				

TABLE 2 (CONT'D)

(d)

VIRTUAL INERTIAS			
EQUATION NUMBER*	QUANTITY	AVERAGE	PERCENT DEVIATION FROM AVERAGE
18, 19	$m_{vir} = 0.2240 \text{ ton-sec}^2/\text{ft}; m_{vir} = 0.2735 \text{ ton-sec}^2/\text{ft}$	0.2488	10
20	$(I_z)_{vir} = 0.3085 \text{ ft-ton-sec}^2$		
21	$(I_x)_{vir} = 1.75 \text{ ft-ton-sec}^2$		
QUANTITY		SOURCE	
DATA**	$\bar{x} = 6.2084 \text{ ft}$ $\rho = 64.15 \text{ lb/ft}^3$ $\bar{y} = 1.1250 \text{ ft}$ $g = 32.17 \text{ ft/sec}^2$ $\bar{z} = 10.1667 \text{ ft}$ $r^2 m_{vir} = s^2 m_{vir} \approx 0$	Reference 4, Table 4	
*See Table 1      **See Notation			

TABLE 2 (CONT'D)

2. STERN PLANES (e)

MEASURED FREQUENCIES (cps) - IN AIR ONLY
20 (predominant)
77
120

(f)

LOGARITHMIC DECREMENT (20 cps)				
DECREMENT*	FIXED PORTION**		MOVABLE PORTION**	
	VALUE	PERCENT DEVIATION FROM AVERAGE	VALUE	PERCENT DEVIATION FROM AVERAGE
$\delta_{\alpha}$	0.0933	- 1.5	0.1098	+17.7
$\delta_{\beta}$	0.0792	-16.4	0.0568	-37.7
$\delta_w$	0.1116	+11.8	0.0971	+ 4.1
$\delta_{\text{modal}}$	----	----	0.1163	+20.6
AVERAGE	0.0947	$\pm 11.9$	0.0933	$\pm 20.4$

\* Because of the orientation of the stern planes  $\delta_{\alpha}$ ,  $\delta_{\beta}$ ,  $\delta_w$  are decrements corresponding to motions  $\alpha$ ,  $\beta$  and  $w$  about the x- and y-axes and along the z-axis, respectively.

\*\*Each stern plane consists of a plane rigidly attached to the hull and to a fixed plane.

TABLE 2 (CONT'D)

USS SAMPSON (DDG-10)

1. RUDDER (g)

MEASURED FREQUENCIES (cps) - IN WATER ONLY
2.18 (predominant)
4.36
7.6
9.0

25

(h)

LOGARITHMIC DECREMENT (2.18 cps)		
DECREMENT*	VALUE	PERCENT DEVIATION FROM AVERAGE
$\delta_{\text{modal}}$	0.02225	-44.8
	0.0582	+44.8
AVERAGE	0.0402	$\pm 44.8$
*See Table 1, Equation [7]		

TABLE 2 (CONT'D)

(i)

DAMPING CONSTANT	
EQUATION NUMBER*	IN WATER (2.18 cps)
16	$C = 0.1479 \text{ ton-sec/ft}$
DATA**	$m_y = 0.8420 \text{ ton-sec}^2/\text{ft}$ $\omega = 2\pi \times 2.18 \text{ sec}^{-1}$ $\delta_v = 0.0402$
<p>* See Table 1                      **<math>m_y = m_a + m_{vir}</math>; <math>m_a = 0.1953</math> was calculated from ship plans and <math>m_{vir}</math> calculated from data in Table 2j. Also <math>\delta_v</math> is approximated by the value of <math>\delta_{\text{modal}}</math>.</p>	

(j)

VIRTUAL MASS		
EQUATION NUMBER*	QUANTITY	
19	$m_{vir} = 0.6467 \text{ ton-sec}^2/\text{ft}$	
	QUANTITY	SOURCE
DATA**	$\bar{x} = 9.9778 \text{ ft}$ $\bar{z} = 9.25 \text{ ft}$ $\rho = 64.15 \text{ lb/ft}^3$ $g = 32.17 \text{ ft/sec}^2$	Ship Plans
<p>* See Table 1                      **See Notation</p>		

## ALBACORE RESULTS

A typical trace taken from ALBACORE records is shown in Figure 4.

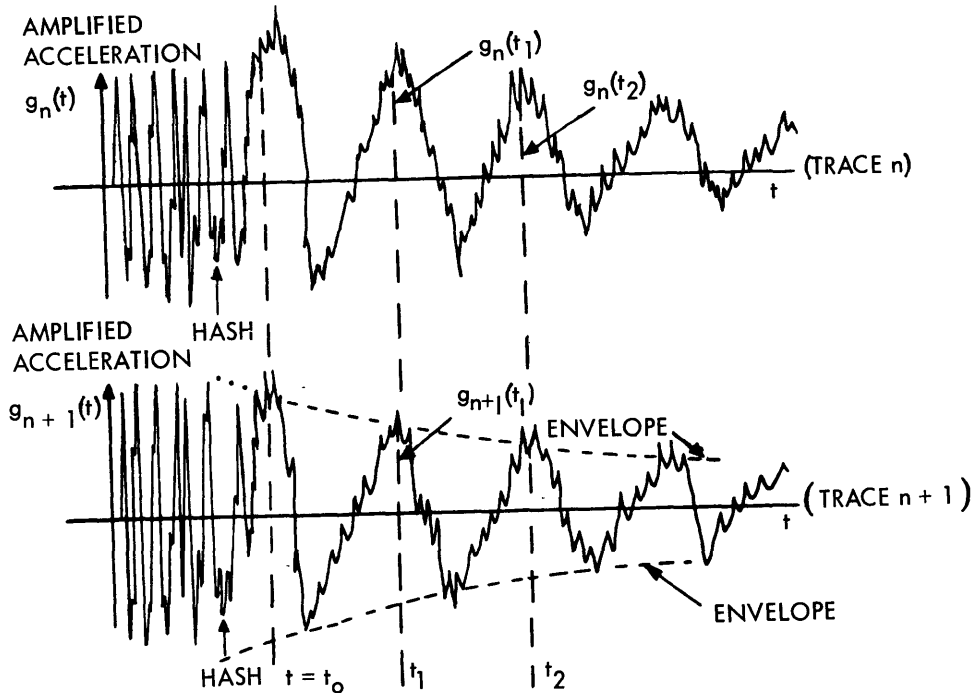


Figure 4. Portion of Oscillogram Record (2 Channels of 12)  
From ALBACORE Rudder Vibration Tests.

Analysis was made for the 20-cps stern plane vibrations (in air), for the 24.5-cps rudder vibration (in air), and for the 13-cps rudder vibration (in water); these are the predominant frequencies. No measurements were made on the submerged stern planes.

Since no hull motions were recorded for which  $\gamma_b$ ,  $\alpha_b$ , and  $v_b$  could be determined, computations for  $\delta_\gamma$ ,  $\delta_\alpha$ , and  $\delta_v$  only were made using Equations [4], [5], [6a] and [6b] of Table 1. Equation [7] was used to compute  $\delta_{\text{modal}}$  for each gage; these values were averaged to give one

value of  $\delta_{\text{modal}}$  for the entire system, i. e., one value for the rudder system and one for the stern plane system.

The records were analysed by fairing a curve through the peak amplitudes of the oscillograms and by measuring peak amplitudes at the same instant of time of all traces obtained from a particular impulsive excitation.\* The faired curves represent the envelope of a decaying sinusoidal wave. Values of  $\gamma$ ,  $\alpha$ , and  $v$  for several peak amplitudes of the trace were obtained by substituting the measured values of  $d_i$  corresponding to fixed times into Equations [1] - [3b]. Ratios of the successive values of  $\gamma$ ,  $\alpha$ , and  $v$  were formed, and the logarithmic decrements for these ratios were computed. Approximately 10 to 15 values for the decrement of  $\gamma$ ,  $\alpha$ , and  $v$  were averaged to yield  $\delta_\gamma$ ,  $\delta_\alpha$ , and  $\delta_v$  from a single record (i. e., single excitation).

Since the rudder and stern plane stocks were not accessible for instrumentation during the tests, the effective lengths of stock,  $l$  and  $l_T$ , could not be computed. Also, values for the hull motions  $\gamma_b$ ,  $\alpha_b$ , and  $v_b$ , required for the computation of  $C$  and  $c$  by Equations [14] and [15], were not available. However, since phase angles between corresponding rudder and hull motions (e. g., between  $v$  and  $v_b$ , etc.) were observed to be immeasurably small, the terms with subscript 2 (e. g.  $\alpha_2$ ,  $\alpha_{b2}$ , etc.) in the right members of these equations may be ignored, thereby reducing

---

\*The peak amplitudes could be measured simultaneously because phase shifts on the rudder were found to be negligible.



the equations to the simpler forms of Equations [16] and [17]. Equation [16] is independent of  $\gamma_b$ ,  $\alpha_b$ , and  $v_b$  as is Equation [17] also if we assume  $\gamma_{b1} = 0$  for convenience of calculation. Under these conditions, damping values C and c in air and in water were computed (see Table 2). In computing the damping values C and c, average values of the decrements  $\delta_v = (\delta_v)_{ave}$  and  $\delta_\gamma = (\delta_\gamma)_{ave}$  are used.

Virtual mass and mass moments of inertia were computed for the rudder using Equations [18] - [21] (see Table 1) and are tabulated in Table 2. Similar results were not obtained for the stern planes since they were tested in air only.

#### SAMPSON RESULTS

Analyses were made on the two most readable records from the SAMPSON trials.<sup>7</sup> Both of these were for in-water trials. In-air testing of the SAMPSON rudder provided no usable data since the lower modes of vibration were not excited sufficiently. Hence no computations were made for virtual mass or virtual mass moments of inertia using Equation [18] which requires in-air frequency data. The total mass of the rudder in translation was obtained by adding the virtual mass computed by Equation [19] to the structural mass.

Plots were made of the total displacement of each gage from both records and are shown in Figure 5. The figure shows that there is no significant rotation of the SAMPSON rudder because all displacements

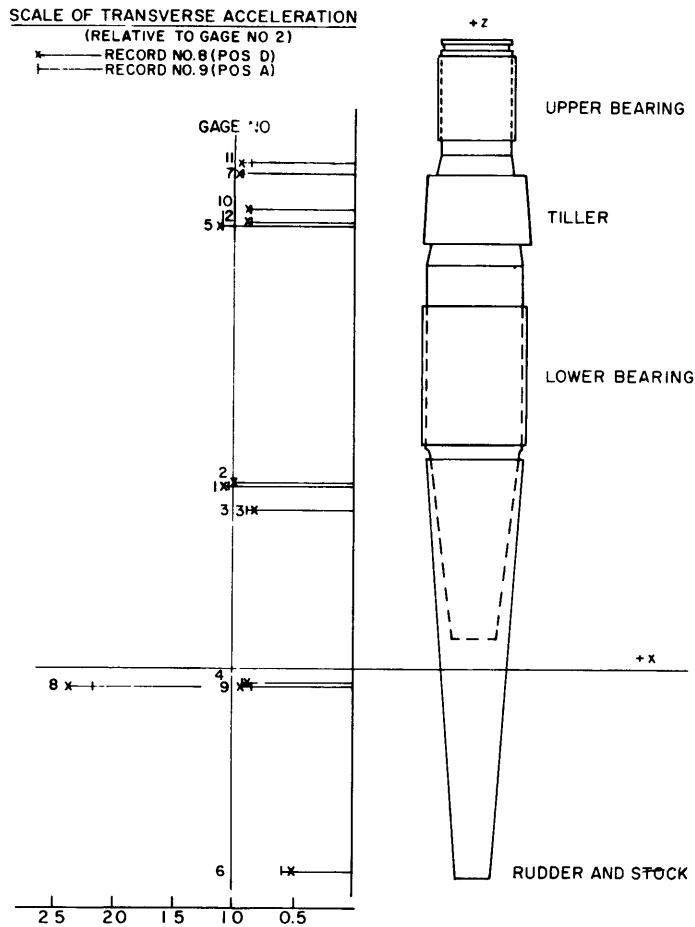


Figure 5. Displacements  $d_i$  Normalized to Gage 2 for 2 Records from SAMPSON Rudder Vibration Tests.

appear to have the same amplitude. As a result, the total motion measured by each gage was not separated into its  $\gamma$ ,  $\alpha$ , and  $\nu$  components.

Further, since the hull displacements were nearly equal to the values of the rudder displacements, hull contributions to the total recorded motion were not extracted. The analysis thus consisted of determining the logarithmic decrement from each gage for both runs. This amounts to determining  $\delta_{\text{modal}}$  for each gage. The results of the analysis for the

predominant frequency of 2.18-cps are presented in Table 2.

## DISCUSSION

Table 2 shows that the procedure developed for computing the logarithmic decrements yields results which do not vary widely. It, therefore, provides reasonable (i. e., order of magnitude) estimates for the decrements and corresponding damping values for the control surfaces useful for ship vibration and flutter analysis. A similar statement may be made for computation of the virtual mass (see Table 2d).

Since the rudder is attached through a flexible stock to a flexible hull, the frequencies in Equation [18] will depend on the mass-elastic properties of the hull as well as on the properties of the rudder-stock system. Apart from hull effects, the frequency data used in Equation [18] correspond to the (measured) coupled  $v$ ,  $\alpha$ ,  $\gamma$  motions of the rudder whereas strict application of Equation [18] requires that frequency data associated with uncoupled cantilevered motions be used (see Appendix E). Nevertheless, transgression of this rigorous application of Equation [18] incurred only a 10 percent deviation from the average of the results obtained by use of Equations [18] and [19]; (see Table 2d).

In general, fluctuations in the results may be largely attributed to difficulty in reading records accurately due to a variety of causes.

For the SAMPSON data, an attempt was made to filter the frequencies of interest from the total recorded signal because so many frequencies were excited. Figures 6a, b are typical traces of SAMPSON records.

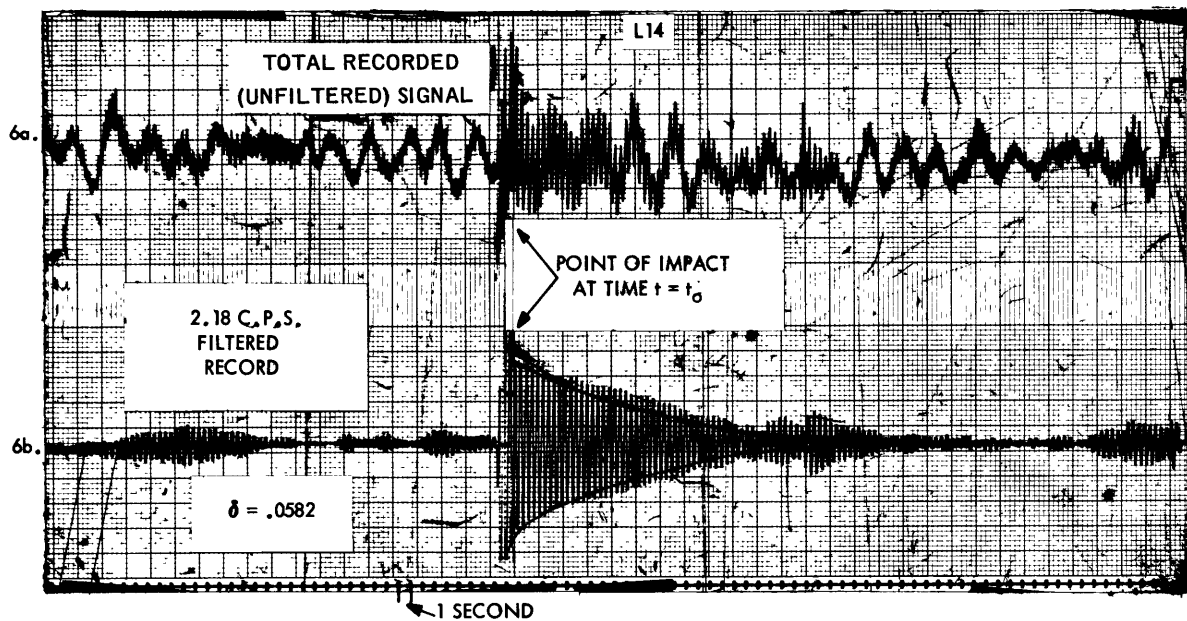


Figure 6a. Total Recorded Signal  
 Figure 6b. Filtered Signal (2.18-cps)

Figure 6. Sample of Accelerometer Data Obtained From One Channel of SAMPSON Tests

Figure 6a shows the total recorded response of a given gage and Figure 6b shows the filtered response; the center frequency of the filter is 2.18-cps. Note that prior to time  $t_0$ , the point in time when the rudder is impulsively excited, a signal of the same frequency, 2.18-cps, occurs in the trace. This signal apparently persists after impact and is superposed upon the decay curve. The source of this signal is uncertain.

We surmise that the predominant signals with the frequency of 2.18-cps correspond to horizontal bending vibration of the hull for the following reasons. The displacements of the rudder and stock and hull are all approximately equal. The hull gage at Location 5 (Figure 1) which is approximately 93 in. forward of the rudder stock recorded approximately

the same response as the rudder stock gages. Moreover, the 2.18-cps frequency is well within the region of lateral vibration of ships, particularly destroyers,<sup>8</sup> whereas the fundamental measured frequencies of some other rudder systems is in the region of 5-8-cps.<sup>9, 10</sup> It should be noted that the fundamental frequency observed for ALBACORE is considerably higher.

Future simplification of data analysis should take advantage of the fact that any decrement  $\delta_i$  can be determined: (1) graphically from oscillographic or magnetically taped records of the signals  $d_1(t)$ ,  $d_2(t)$  etc., or by (2) devising electrical circuitry to record the values of the decrements directly either as soon as the signals are measured or in the laboratory using tape stored signal data.

### CONCLUSIONS

Based on the foregoing analysis and test results, the following conclusions have been reached:

1. It appears likely that reliable results for damping coefficients and inertial parameters for control surfaces can be obtained using the methods presented here.

2. Use of modal analysis equipment (filters) which gives the frequency, logarithmic decrement, and damping for each mode and the relative phase between any two vibratory displacements at different points on a structure, for a particular mode, is vital for the practical application of the present analysis.<sup>11-14</sup>

3. The test procedure must be improved. Impulsive loading should be controlled so that all significant modal frequencies of the control surfaces are excited (see Discussion). Extraneous noise and vibration effects on the recorded data must be eliminated or minimized by controlling the source of the trouble and/or improving the instrumentation.

#### RECOMMENDATIONS

1. Further tests on control surfaces of surface ships, submarines, hydrocrafts, etc. should be conducted in accordance with the procedure presented here to obtain realistic damping and inertial parameters for these surfaces.

2. The analysis should be extended to include the mass-elastic effects of tiller connections, links, and other steering gear machinery on the vibrational response of the system.

3. Analysis equipment should be developed or purchased in order to obtain the desired results from the recorded data.

#### ACKNOWLEDGMENTS

The authors are grateful to Mr. G. Franz, Mr. E. Noonan and Dr. E. Buchmann for constructive criticism. Dr. Buchmann also helped in the planning of the tests. The authors wish to express their appreciation to Mr. R. Price for conducting the vibration test on ALBACORE and to Mr. R. M. Murray for conducting the vibration test on SAMPSON. We are also grateful for the assistance of LCDR W. A. Greene, Captain of

the ALBACORE, and his crew and of Cdr. F. W. Isen, Captain of the SAMPSON, and his crew in conducting these tests. Mr. Max Morris reduced the damping data for ALBACORE, and Mr. Ed Hoyt evaluated the damping data for SAMPSON.

## APPENDIX A

### DEVELOPMENT OF EQUATIONS FOR DETERMINATION OF RUDDER MOTIONS $\gamma$ , $\alpha$ , $v$

Figure 1 is a diagram of the gage layout on the rudder. The gages are placed along x-, z-axes whose origin is at the center of mass of the rudder.\* Thus,  $x_1$  is the distance between the center of mass and Gage 4 which measures displacement  $d_4$ . It is assumed that no  $\alpha$  contribution to the total measured motion of a gage exists on the horizontal axis (x-axis) through the center of mass. Likewise, no  $\gamma$  contribution to the total measured motion of a gage exists on the vertical axis (z-axis) through the center of mass. Only motions in the  $\gamma$ ,  $\alpha$ , and  $v$  degrees of freedom contribute significantly to the total coupled athwartship motion of the rudder. Referring to Figure 1,

$$d_4 = v + x_1 \gamma$$

$$d_8 = v - x_2 \gamma$$

from which

$$\gamma = \frac{1}{x_1 + x_2} (d_4 - d_8) = K_1 (d_4 - d_8) \quad [A-1]$$

---

\*Prior to the conduction of the test, the centers of mass of the rudder in air and in water must be computed. The center of mass in water is computed to be the center of mass of the combined rudder-rudder stock system including the virtual mass which is approximated by the volume of water contained in an ellipsoidal cylinder of revolution taken about a rudder axis (see Reference 4, page 12). The virtual mass computed in accordance with the method of this reference (Equation [19], Table 1) may be compared with the experimental value determined from the data by use of Equation [18], Table 1.



where  $K_1 = \frac{1}{x_1+x_2} = \text{constant}$

likewise  $d_2 = v - z_1 \alpha$

from which  $\alpha = \frac{1}{z_1+z_2} (d_6 - d_2)$

$$= K_2 (d_6 - d_2) \quad [\text{A-2}]$$

where  $K_2 = \frac{1}{z_1+z_2} = \text{constant}$

From the equations leading to [A-1] and [A-2] we have

or  $v = K_3 (d_2 + K_4 d_6) \quad [\text{A-3a}]$

$$v = K_5 (d_4 + K_6 d_8) \quad [\text{A-3b}]$$

where  $K_3 = \frac{z_2}{z_1+z_2}$

$$K_4 = z_1/z_2$$

$$K_5 = \frac{x_2}{x_1+x_2}$$

$$K_6 = x_1/x_2$$

## APPENDIX B

### DETERMINATION OF EFFECTIVE LENGTHS OF CONTROL SURFACE STOCK

Assume a set of cartesian coordinate axes ( $x'$ -,  $y'$ -,  $z'$ -) with the origin  $0'$  at the point of attachment of the control surface to the stock (usually at the top of the control surface) such that the  $z'$ -axis runs through the center of the control surface stock (see Figure 7); note  $z' = z - b$  and  $x' = x - h$ . For simplicity, we will call our control surface a rudder. All equations and statements apply equally well to stern planes.

Referring to Figure 8, define  $(d_{v, \alpha})_{7-11}$  as the displacement of the stock between Gage Positions 7 and 11 due to the  $\alpha$  and  $v$  motions of the stock. Also, let  $\gamma_{7-11}$  be the  $\gamma$  rotation of the stock between Gage Positions 7 and 11. Then,

$$d_7 = (d_{v, \alpha})_{7-11} + x_7 \gamma_{7-11} \quad [B-1]$$

$$d_{11} = (d_{v, \alpha})_{7-11} - x_{11} \gamma_{7-11} \quad [B-2]$$

From [B-1] and [B-2], noting that  $x_7 = x_{11}$ , we have

$$\gamma_{7-11} = K_7 (d_7 - d_{11}) \quad [B-3]$$

where

$$K_7 = \frac{1}{2x_7} = \frac{1}{2x_{11}} = \text{constant}$$

Similarly

$$d_{12} = (d_{v, \alpha})_{10-12} + x_{12} \gamma_{10-12} \quad [B-4]$$

$$d_{10} = (d_{v, \alpha})_{10-12} - x_{10} \gamma_{10-12} \quad [B-5]$$

from which (since  $x_{10} = x_{12}$ ),

$$\gamma_{10-12} = K_8 (d_{10} - d_{12}) \quad [B-6]$$

where

$$K_8 = \frac{1}{2x_{10}} = \frac{1}{2x_{12}} = \text{constant}$$

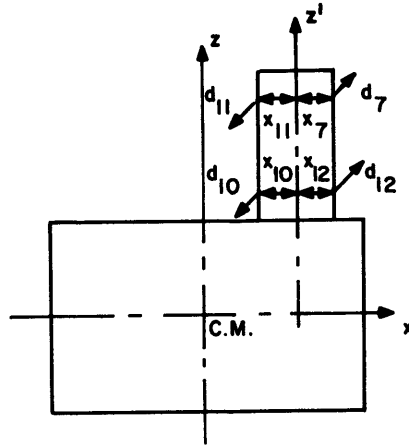
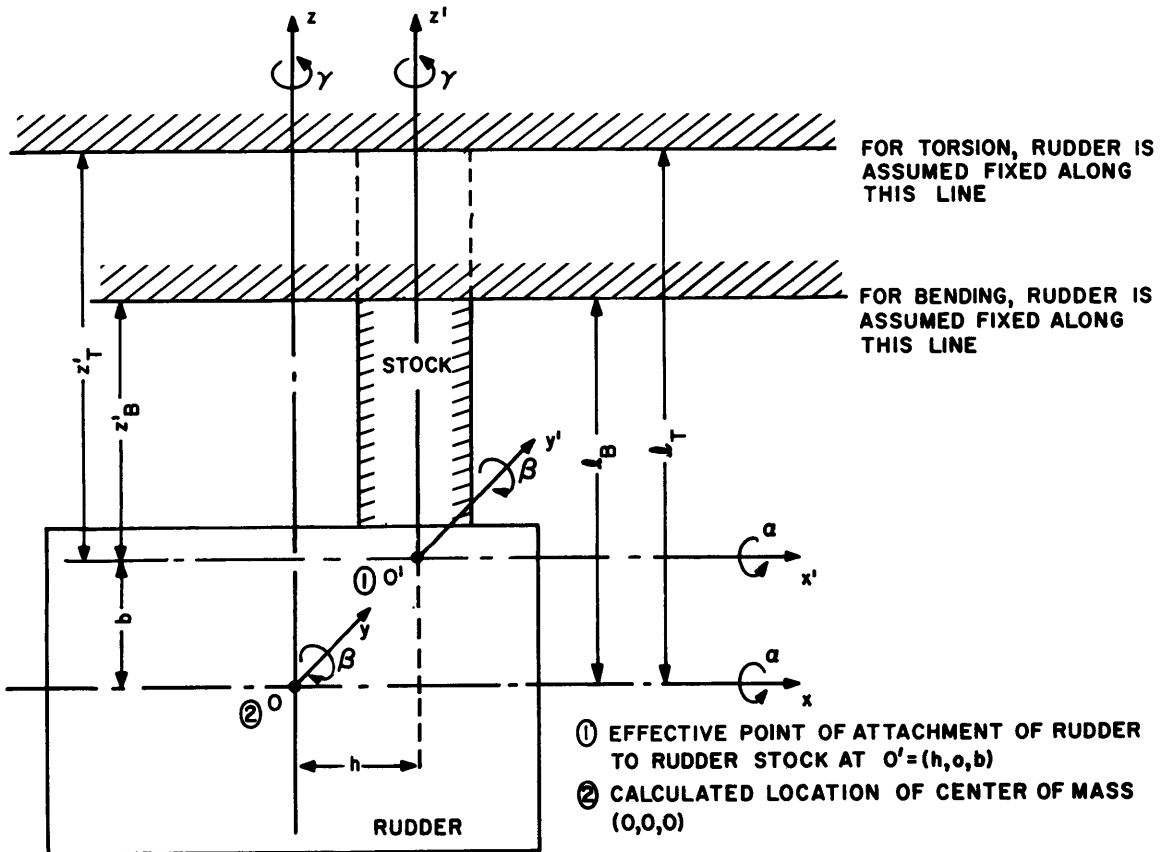


Figure 7a. Location of Gages Used to Record Rudder Stock Motions.



Note:  $O'$  is displaced from top of stock in this figure to indicate rudder-rudder attachment is necessarily at top of rudder.

Figure 7b. Rudder Axes.

Figure 7. Rudder Coordinates and Locations of Gages.

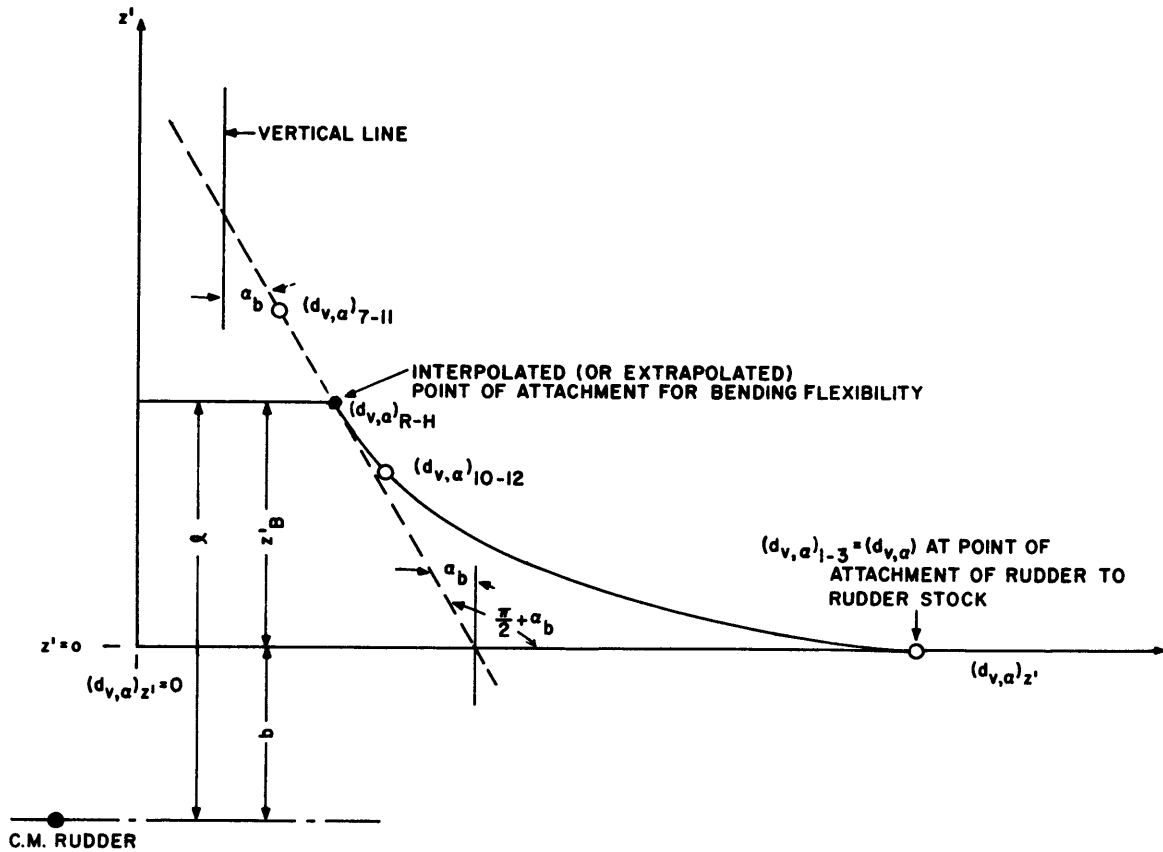


Figure 8. Curve for Determination of Effective Length of Stock for Bending Motion.

From Equations [ B-1], [ B-2], [ B-4], and [ B-5] we obtain

$$(d_{v,\alpha})_{7-11} = \frac{1}{2} (d_7 + d_{11}) \quad [ B-7]$$

$$(d_{v,\alpha})_{10-12} = \frac{1}{2} (d_{10} + d_{12}) \quad [ B-8]$$

From Figure 1,  $d_3 = (d_{v,\alpha})_{1-3} + x_5 \gamma_{1-3}$  [ B-9]

and  $d_1 = (d_{v,\alpha})_{1-3} - x_6 \gamma_{1-3}$  [ B-10]

From Equations [ B-9], and [ B-10] we have

$$\gamma_{1-3} = K_{14} (d_3 - d_1) \quad [ B-11]$$

and  $(d_{v,\alpha})_{1-3} = K_{12} (d_3 + K_{13} d_1)$  [ B-12]

where 
$$K_{12} = \frac{x_6}{x_5 + x_6} = \text{constant}$$

and 
$$K_{13} = \frac{x_5}{x_6} = \text{constant}$$

$$K_{14} = \frac{1}{x_5 + x_6} = \text{constant}$$

Figures 8 and 9 are plots of  $(d_{v,\alpha})_{z'}$  and  $\gamma$  versus  $z'$  respectively obtained from the values calculated by the above equations. For a rigid control surface,  $\gamma$  has a constant value, i. e., the value of  $\gamma$  obtained by Equation [A-1] should equal that obtained by Equation [B-11]. Both  $(d_{v,\alpha})_{1-3}$  and  $\gamma_{1-3}$  are plotted at  $z' = 0$ .

In Figure 8, the curve of  $(d_{v,\alpha})$  against  $z'$  approaches the straight line whose slope is the tangent of  $\frac{\pi}{2} + \alpha_b$ . This line appears as the dotted line in Figure 8. The angle this makes with the vertical (parallel to  $z'$ ) is  $\alpha_b$ . The method of measuring  $\alpha_b$  and the location of this line in the plane will be discussed later in this appendix. These straight lines (or asymptotes) remain straight for increasing  $z'$  since they represent the rigid body motions and torsional motions of the hull. Bending of the hull in the horizontal plane would give rise to additional curvature of the curve in Figure 8 at a value of  $z'$  in the vicinity of the hull.

The quantities  $\gamma_b$ ,  $z'_T$ , and  $z'_B$  are measured from the plots of Figures 8 and 9;  $z'_T$  and  $z'_B$  are the distances from the point of attachment of the rudder stock to rudder (usually, although not always, at the top of the rudder) to the point of attachment of stock to hull in torsion and

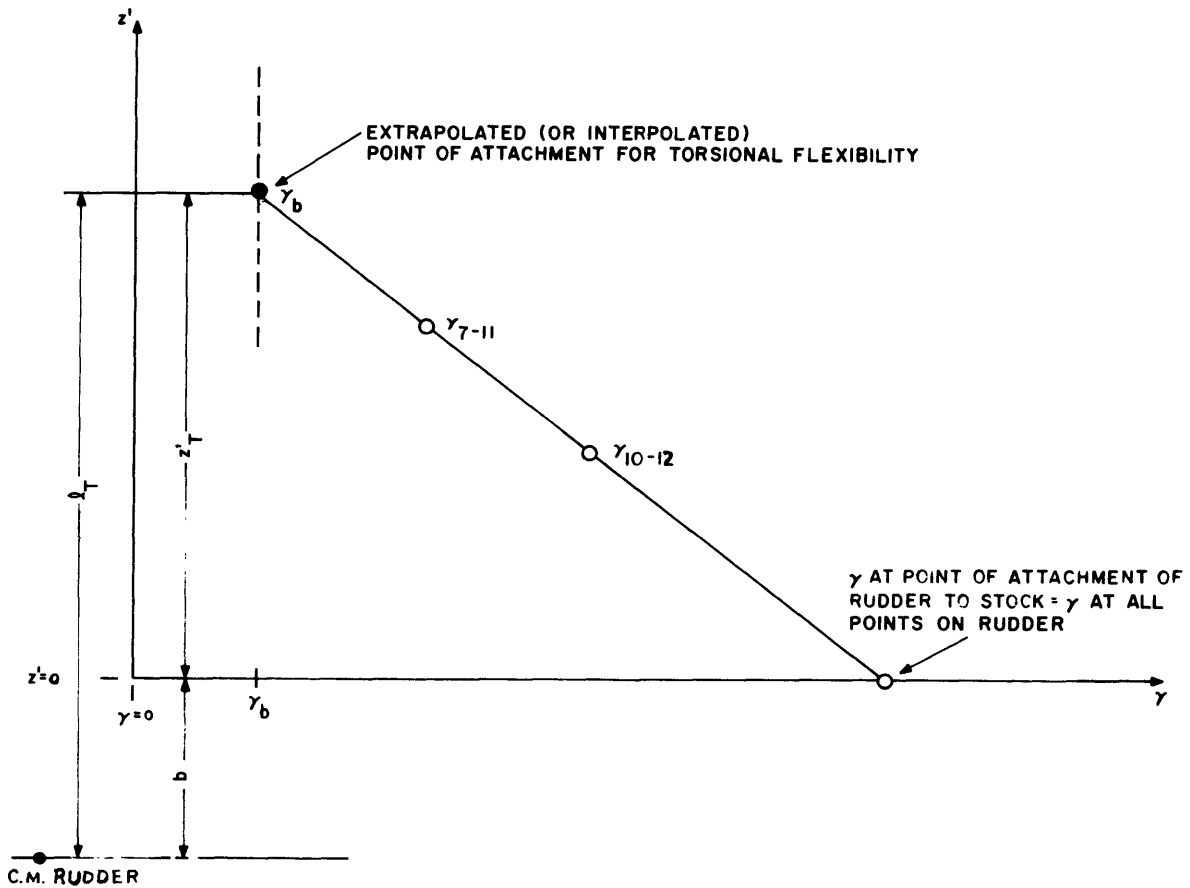


Figure 9. Curve for Determination of Effective Length of Stock for Rotational Motion (Torsion).

bending, respectively. The measured values of  $\gamma$  will be used in subsequent calculations.

When  $\gamma$  is plotted against  $z'$ , it is expected that a point will be reached at which the curve is vertical. The value of  $\gamma$  at this point will be called  $\gamma_b$ . The quantity  $l_T$  is the distance along  $z'$  from the point on  $z'$  where  $\gamma = \gamma_b$  to the center of mass of the rudder. It is computed by measuring  $z'$  from  $z' = 0$  to  $z'$  at  $\gamma = \gamma_b$  and adding the quantity  $b$  (see Figures 8 and 9) to this result, i. e.,  $l_T = z'_T + b$ .

In the plot of  $d_{v,\alpha}$  versus  $z'$ , note that the point where the curve  $d_{v,\alpha}$  versus  $z'$  becomes linear is the point of attachment of the rudder stock to the hull in bending. The value of  $d_{v,\alpha}$  at this point, which is obtained by extrapolation (or interpolation), will be called  $(d_{v,\alpha})_{R-H}$ . The linear portion of the curve makes an angle  $\alpha_b$  with the vertical (see Figure 8);  $\alpha_b$  will be determined below. The value of  $\ell$  is the distance along  $z'$  from the point on  $z'$  where  $d_{v,\alpha} = (d_{v,\alpha})_{R-H}$  to the center of mass of the rudder. It is computed by measuring  $z'_B$  from  $z' = 0$  to  $z'$  at  $d_{v,\alpha} = (d_{v,\alpha})_{R-H}$  and adding the quantity  $b$  (see Figures 7 and 8) to this result, i. e.,  $\ell = z'_B + b$ .

The hull angle of torsion, represented by  $\alpha_b$ , may be determined by the following method (see Figures 2 and 10).

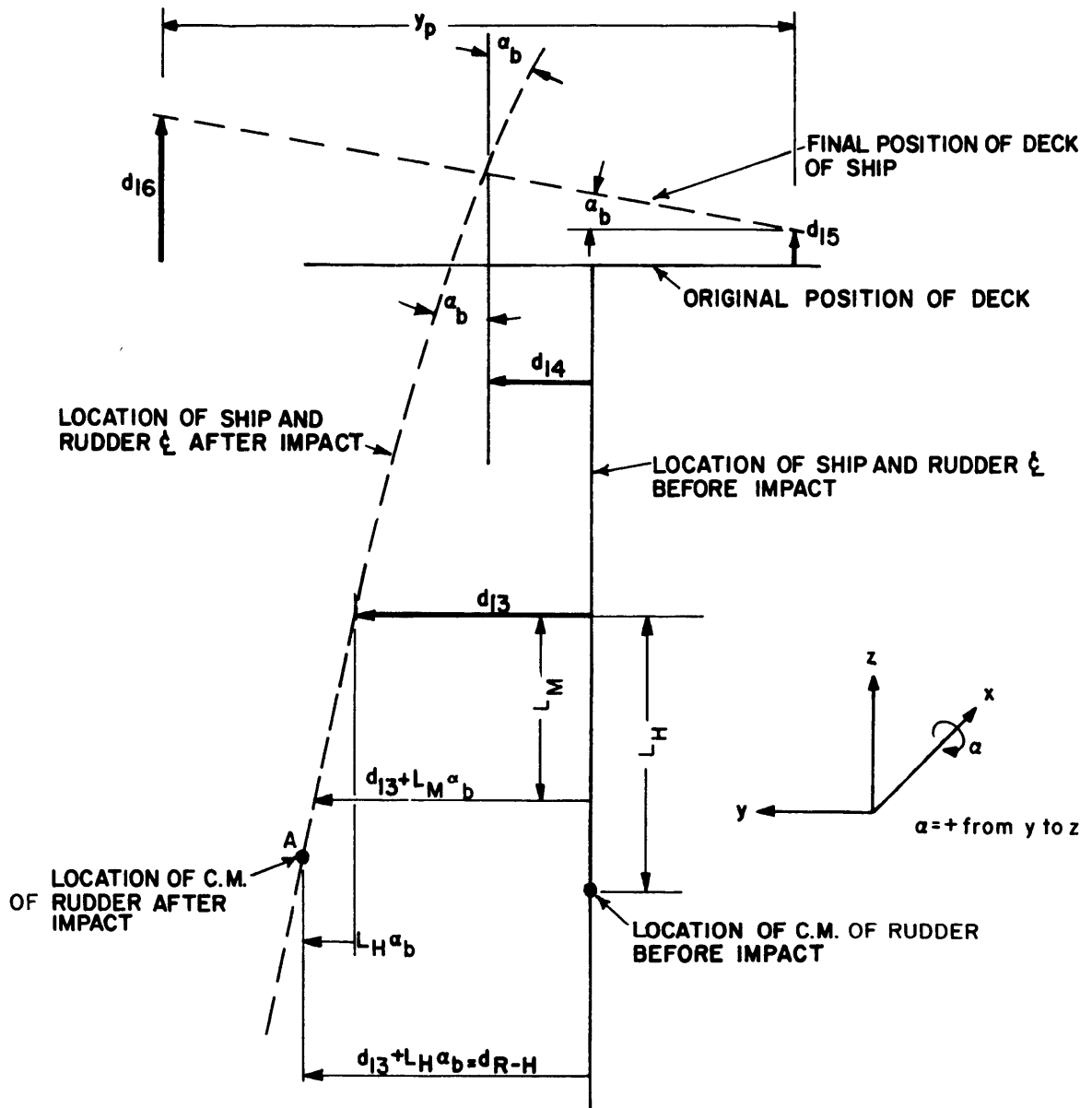
The ship is instrumented with two accelerometers (Gages 13 and 14) to measure the athwartship motions of the section of the hull in line with the rudder stock and two accelerometers (Gages 15 and 16) to measure the vertical motions of the hull in the transverse plane which contains the rudder stock. In Figure 10 let,

$L_P$  = vertical distance between Gage Locations 13 and 14,

$L_H$  = vertical distance between Gage Location 13 and the center of mass of the rudder,

$Y_P$  = horizontal distance between Gage Locations 15 and 16, and

$d_{13}, d_{14}, d_{15}, d_{16}$ , = displacements of the hull at Gage Locations 13, 14, 15, and 16, respectively.



NOTE 1: The figure does not show the  $\gamma$  dependency [see Equations (B-15)-(B-18)].

NOTE 2:  $L_M >$  or  $<$   $L_H$ .

Figure 10. Motion of Hull and Rudder, with No Relative Motion between Rudder and Hull



The solid line in Figure 10 represents the undisturbed position of the ship and the dotted line represents the horizontal torsion-bending motions of the ship after impact on the control surface, assuming the control surface-stock system remains completely rigid with respect to the hull, so that the motion of the control surface due to the motion of the hull may be determined.

Then 
$$\alpha_b = \frac{(d_{13} \quad -d_{14})}{L_P} \quad [B-13]$$

and 
$$\alpha_b = \frac{(d_{16} \quad -d_{15})}{\bar{y}_P} \quad [B-14]$$

This value of  $\alpha_b$  determines the slope of the linear part of the curve in Figure 8. Hence, the displacement of the center of mass of the control surface due to the coupled torsion-horizontal-bending motions of the hull is given by (see Figure 10);

$$d_{R-H} = d_{13} + L_H \alpha_b - h \gamma_b \quad [B-15]$$

Substituting Equation [B-13] into the above expression, Equation

[B-15] may be written as

$$\begin{aligned} d_{R-H} &= d_{13} + \frac{L_H}{L_P} (d_{13} \quad -d_{14}) - h \gamma_b \\ &= \left( 1 + \frac{L_H}{L_P} \right) d_{13} - \frac{L_H}{L_P} d_{14} - h \gamma_b \end{aligned}$$

or 
$$d_{R-H} = K_9 d_{13} - K_{10} d_{14} - h \gamma_b \quad [B-16]$$

where

$$K_9 = 1 + \frac{L_H}{L_P} = 1 + K_{10} = \text{constant}$$

$$K_{10} = \frac{L_H}{L_P} = \text{constant}$$

Also, by using Equation [B-14],

$$d_{R-H} = d_{13} + L_H \frac{(d_{16} - d_{15})}{y_P} - h \gamma_b$$

or

$$d_{R-H} = d_{13} + K_{11} (d_{16} - d_{15}) - h \gamma_b \quad [B-17]$$

where

$$K_{11} = \frac{L_H}{y_P} = \text{constant}$$

In determining the motion of the rudder relative to the hull in the y-direction when a flexible stock is considered, the displacement of the hull must be accounted for because the displacement on the hull is included in the rudder motions measured by the gages on the rudder. Referring to Figure 10, we may define the motion of rudder relative to the hull at the M<sup>th</sup> gage position by

$$d_{M_R} = d_M - (d_{13} + L_M \alpha_b - x_M \gamma_b) \quad [B-18]$$

where  $d_M$  is the motion of the M<sup>th</sup> gage which includes the contribution of the hull motions as well as the effects of rudder stock flexibility and where  $L_M$  is the vertical distance between the M<sup>th</sup> gage and Gage 13 and  $x_M$  is the horizontal distance between the M<sup>th</sup> gage and the rudder stock ( $x_M$  is positive when the M<sup>th</sup> gage is aft of the stock and negative if forward of

the stock). \* If the contribution of the term  $x_M \gamma_b$  is negligible, the following expression may be used:

$$d_{M_R} = d_M - (d_{13} + L_M \alpha) \quad [B-19]$$

---

\*When the  $M^{\text{th}}$  gage is at the center of mass, the term in parenthesis in Equation [B-18] reduces the right hand side of Equation [B-15].

## APPENDIX C

### DETERMINATION OF LOGARITHMIC DECREMENTS

In determining the motion of the center of mass of the rudder relative to the hull in the y-direction, the displacement of the hull must be accounted for ( in addition to the displacement of the center of mass associated with the elasticities of the flexible stock) because it is included in the rudder motions measured by the gages on the rudder. Thus rudder motion relative to the hull motion in the y degree of freedom is

$$v - d_{R-H} = v - (d_{13} + L_H \alpha_b) . *$$

This is equivalent to the motion of the center of mass of the rudder attached through a flexible stock to a rigid hull.

The values for  $\gamma_b$ ,  $\alpha_b$ , and  $d_{R-H}$  must be subtracted from the recorded  $\gamma$ ,  $\alpha$ , and  $v$  motions of the rudder to obtain the true rudder relative to hull motion.

The logarithmic damping decrement for a motion A (t) is

$$\delta_A = \frac{1}{q} \log_e \left[ \frac{A_{t_0}}{A_{t_0 + q\tau}} \right] \quad [C-1]$$

where

$A_{t_0}$  = the value of A at time  $t=t_0$

$A_{t_0 + q\tau}$  = the value of A at time  $t=t_0 + q\tau$

where  $\tau$  is the period of oscillation and q is an integer equal to the total number of periods of oscillation of A between the measured amplitudes

---

\*In Equation [ B-18],  $d \rightarrow v$ ,  $L \rightarrow L_H$ , and the term  $x \gamma_b$  has been neglected for the present application.

(see Figure 11). Similar relationships hold for the motions  $\gamma(t)$ ,  $\alpha(t)$  and  $v(t)$ .

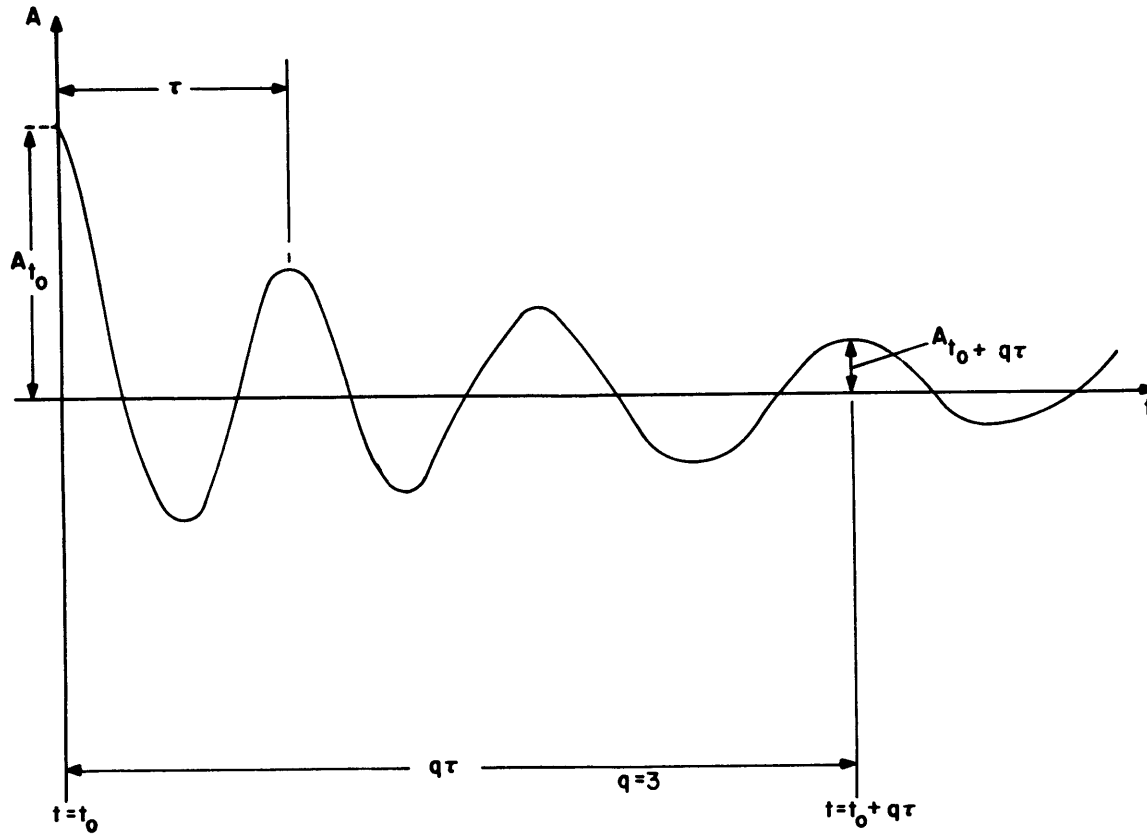


Figure 11. Sinusoidal Wave Form Showing Decay due to Viscous Damping.

We define the logarithmic decrement of the  $\gamma$  motion of the rudder relative to the hull by

$$\delta_{\gamma_R} = \frac{1}{q} \log_e \frac{[\gamma - \gamma_b]_{t=t_0}}{[\gamma - \gamma_b]_{t=t_0 + q\tau}} \quad [C-2]$$

the logarithmic decrement of the  $\alpha$  motion of the rudder relative to the hull by

$$\delta_{\alpha_R} = \frac{1}{q} \log_e \frac{[\alpha - \alpha_b]_{t=t_0}}{[\alpha - \alpha_b]_{t=t_0 + q\tau}} \quad [C-3]$$

and the logarithmic decrement of the  $v$  motion of the rudder relative to the hull by

$$\delta_{v_R} = \frac{1}{q} \log_e \frac{[v - d_{R-H}]_{t=t_0}}{[v - d_{R-H}]_{t=t_0 + q\tau}} \quad [C-4]$$

In terms of displacement, these Equations [C-2], [C-3], and [C-4] respectively become Equations [10], [11], and [12] of Table 1.

Similarly, the decrement of the relative motion of the  $M^{\text{th}}$  location on the rudder is given by (see Equation [13] of Table 1)

$$\delta_{M(\text{modal})_R} = \frac{1}{q} \log_e \left\{ \frac{[d_M - (d_{13} + L_M \alpha_b - x_M \gamma_b)]_{t=t_0}}{[d_M - (d_{13} + L_M \alpha_b - x_M \gamma_b)]_{t=t_0 + q\tau}} \right\} \quad [C-5]$$

In these equations,  $d_M$  is the recorded displacement of the rudder at the  $M^{\text{th}}$  position and  $L_M$  is the vertical distance of the  $M^{\text{th}}$  position to the gage where the displacement  $d_{13}$  is measured.

For some applications, the term  $x_M \gamma_b$  may be negligible. In the present application to ALBACORE and SAMPSON, the terms  $d_{13} + L_M \alpha_b - x_M \gamma_b$  were not considered (see Results) so that Equation [C-5] reduces to Equation [7] of Table 1.

Theoretically  $\delta_{v_R} = \delta_{\gamma_R} = \delta_{\alpha_R} = \delta_{\text{modal}}$ . The analysis of the record should verify this assertion.

APPENDIX D

DERIVATION OF EQUATIONS FOR PARAMETERS C AND c

Derivation of Equations [ 14] and [ 15] of Table 1 are presented in this Appendix.

Consider Equation [ 62a] of Reference 1. At zero ship speed, this is (see Notation):

$$M_y \ddot{v} = -12k_s \left[ v - v_b + h\gamma - b\alpha - \frac{1}{2} t(\alpha + \alpha_b) \right] - C\dot{v}$$

$$C = \frac{-M \ddot{v} - 12k_s \left[ v - v_b + h\gamma - b\alpha - \frac{1}{2} t(\alpha + \alpha_b) \right]}{\dot{v}}$$

Suppose the motion in each degree of freedom is a damped sinusoid.

Then\*

$$v = v_1 e^{\mu t} \sin \omega t$$

$$\alpha = e^{\mu t} (\alpha_1 \sin \omega t + \alpha_2 \cos \omega t)$$

$$\gamma = e^{\mu t} (\gamma_1 \sin \omega t + \gamma_2 \cos \omega t)$$

$$v_b = e^{\mu t} (v_{b1} \sin \omega t + v_{b2} \cos \omega t)$$

$$\alpha_b = e^{\mu t} (\alpha_{b1} \sin \omega t + \alpha_{b2} \cos \omega t)$$

$$\gamma_b = e^{\mu t} (\gamma_{b1} \sin \omega t + \gamma_{b2} \cos \omega t)$$

where  $\alpha_1, \alpha_2, \gamma_1, \gamma_2, v_{b1}, v_{b2}, \alpha_{b1}, \alpha_{b2}, \gamma_{b1}, \gamma_{b2}$  are constants.

\*It may be desirable in future calculations or measurements to express

these equations in the following alternative forms:

$v = Ve^{\mu t} \sin \omega t$	$V = v_1$	$\phi_1 = \tan^{-1} \left( \frac{\alpha_2}{\alpha_1} \right)$
$\alpha = Ae^{\mu t} \sin (\omega t + \phi_1)$	$A = \sqrt{\alpha_1^2 + \alpha_2^2}$	$\phi_2 = \tan^{-1} \left( \frac{\gamma_2}{\gamma_1} \right)$
$\gamma = \Gamma e^{\mu t} \sin (\omega t + \phi_2)$	$\Gamma = \sqrt{\gamma_1^2 + \gamma_2^2}$	$\phi_3 = \tan^{-1} \left( \frac{v_{b2}}{v_{b1}} \right)$
$v_b = V_b e^{\mu t} \sin (\omega t + \phi_3)$ etc.	$V_b = \sqrt{v_{b1}^2 + v_{b2}^2}$ etc.	etc.

The exponent  $\mu$ , the frequency  $\omega$ , and the constants  $\alpha_1$ ,  $\alpha_2$ , etc. can all be determined from records. Moreover,

$$\begin{aligned}\dot{v} &= v_1 (\mu \sin \omega t + \omega \cos \omega t) e^{\mu t} \\ \dot{v} &= v_1 [(\mu^2 - \omega^2) \sin \omega t + 2\mu\omega \cos \omega t] e^{\mu t} \\ \ddot{a} &= \left\{ \left[ \alpha_1 (\mu^2 - \omega^2) - 2\alpha_2 \mu \omega \right] \sin \omega t + \left[ \alpha_2 (\mu^2 - \omega^2) + 2\alpha_1 \mu \omega \right] \cos \omega t \right\} e^{\mu t} \\ \ddot{\gamma} &= \left\{ \left[ \gamma_1 (\mu^2 - \omega^2) - 2\gamma_2 \mu \omega \right] \sin \omega t + \left[ \gamma_2 (\mu^2 - \omega^2) + 2\gamma_1 \mu \omega \right] \cos \omega t \right\} e^{\mu t} \\ \dot{\gamma} &= \left[ (\gamma_1 \mu - \gamma_2 \omega) \sin \omega t + (\gamma_1 \omega + \gamma_2 \mu) \cos \omega t \right] e^{\mu t} \\ \dot{\gamma}_b &= \left[ (\gamma_{b1} \mu - \gamma_{b2} \omega) \sin \omega t + (\gamma_{b1} \omega + \gamma_{b2} \mu) \cos \omega t \right] e^{\mu t}\end{aligned}$$

Substituting the appropriate variable  $\dot{v}, \dot{v}, v, v_b, \gamma, \alpha, \alpha_b$  in the equation for C, we find at time

$$t = \frac{2n\pi}{\omega} ; n = 0, 1, 2, \dots$$

$$C = -2M_y \mu + \frac{12k_s}{v_1 \omega} \left[ v_{b2} - h\gamma + b\alpha_2 + \frac{\ell}{2} (\alpha_2 + \alpha_{b2}) \right]$$

Similarly from Equation [62b] of Reference 1 (see Notation)

$$\begin{aligned}I_z \ddot{\gamma} - I_{xz} \ddot{a} &= -12k_s h (v - v_b) + 6k_s h (\ell + 2b) \alpha - \left[ \frac{GJe}{\ell_T} + 12k_s h^2 \right] \gamma \\ &+ 6k_s h \ell \alpha_b + \frac{GJe}{\ell_T} \gamma_b - c (\dot{\gamma} - \dot{\gamma}_b)\end{aligned}$$

or

$$c = \left[ \frac{1}{\dot{\gamma} - \dot{\gamma}_b} \right] \left\{ -I_z \ddot{\gamma} + I_{xz} \ddot{a} - 12k_s h (v - v_b) + 6k_s h (\ell + 2b) \alpha - \left[ \frac{GJe}{\ell_T} + 12k_s h^2 \right] \gamma + 6k_s h \ell \alpha_b + \frac{GJe}{\ell_T} \gamma_b \right\}$$



Substituting the appropriate variables  $\ddot{\gamma}$ ,  $\ddot{\alpha}$ ,  $v$ ,  $v_b$ ,  $\alpha$ ,  $\gamma$ ,  $\alpha_b$ ,  $\gamma_b$  in the equation for  $c$ , we find at time

$$t = \frac{2n\pi}{\omega} \quad ; \quad n = 0, 1, 2, \dots$$

$$c = \left[ \frac{1}{(\gamma_1 - \gamma_{b1})\omega + (\gamma_2 - \gamma_{b2})\mu} \right] \left\{ -I_z \left[ \gamma_2(\mu^2 - \omega^2) + 2\gamma_1\mu\omega \right] \right.$$

$$\left. + I_{xz} \left[ \alpha_2(\mu^2 - \omega^2) + 2\alpha_1\mu\omega \right] + 12k_s h \left[ v_{b2} - h\gamma_2 + b\alpha_2 + \frac{\ell}{2} (\alpha_2 + \alpha_{b2}) - \frac{GJe}{\tau} (\gamma_2 - \gamma_{b2}) \right] \right\}$$

In these equations,  $-\frac{\mu}{\omega} = \frac{\delta}{2\pi} = \frac{C}{C_c} = \frac{c}{c_c}$  (see Reference 3) where  $\delta$  is the logarithmic decrement of the waveform,  $\mu$  is the real part of  $\lambda$  indicating the degree of damping and  $\omega$  is the imaginary part of  $\lambda$  which is the circular frequency of vibration. Here  $C_c$  and  $c_c$  are critical damping constants for the translational and rotational degrees of freedom, respectively. It should be clear that  $\delta$ ,  $\omega$ , (and hence  $\mu$ ) are directly obtainable from the waveforms for a particular mode of vibration as are the constants  $v_{b2}$ ,  $\gamma_2$ ,  $\alpha_2$ , etc. Thus,  $C$  and  $c$  are determined from measured and calculated data.

## APPENDIX E

### DETERMINATION OF VIRTUAL MASS AND MASS MOMENTS OF INERTIA

Methods for determining the virtual mass and virtual mass moments of inertia are given in this Appendix.

In order to obtain "ball park" values for the frequencies of the rudder by means of a simple computation, let us assume first that we are treating a two degree-of-freedom system, consisting of  $v$ - and  $\gamma$ - motions, i. e.,  $\alpha$ - motions are neglected. With this approach, two types of calculations can be made. The simpler type of calculation treats the system as uncoupled, whereas the second type which involves a bit more computation, treats the system as a coupled one.<sup>9\*</sup>

Equations developed for determining the frequencies associated with uncoupled motions in two degrees of freedom,  $v$ - translation and  $\gamma$ - rotation, are given in Reference 9, page 321. The frequencies associated with uncoupled motions are inversely proportional to the mass and mass moments of inertia, respectively. The equations for the frequencies associated with uncoupled  $v$ - and  $\gamma$ - motions are

$$f_v = \frac{1}{2\pi} \sqrt{\frac{3EI_P}{2m_y l^3}} \quad \text{and} \quad f_\gamma = \frac{1}{2\pi} \sqrt{\frac{GI_P}{l I_z}} \quad [E-1]$$

---

\*For example, the numerical values for the parameters of the "barn door" type rudder of Reference 9 indicate that the maximum difference in the corresponding frequencies obtained from the use of these two types is not likely to exceed 35 percent for one of the modes and 20 percent for the other mode.

which may be written as

$$f_v \propto m_y^{-1/2} \quad \text{and} \quad f_\gamma \propto I_z^{-1/2} \quad [E-2]$$

where, in general (i. e., for any medium),  $f_v$  is the frequency of the translational motion and  $f_\gamma$  is the frequency of the rotational motion,  $m_y$  is the total mass\* of the rudder,  $I_z$  is the mass moment of inertia of the rudder about the rudder stock axis, and  $I_p$  is the polar moment of inertia of the rudder stock.

In air

$$f_{v,a} = \frac{1}{2\pi} \sqrt{\frac{3EI}{2m_a \ell^3}}, \quad f_{\gamma,a} = \frac{1}{2\pi} \sqrt{\frac{GI}{\ell_t (I_z)_a}} \quad [E-3]$$

or

$$f_{v,a} \propto m_a^{-1/2}, \quad f_{\gamma,a} \propto (I_z)_a^{-1/2} \quad [E-4]$$

where  $f_{v,a}$  is the frequency associated with translational motion (only) in air and  $f_{\gamma,a}$  is the frequency associated with  $\gamma$  rotation (only) in air.

Similarly

$$f_{v,w} \propto m_y^{-1/2}, \quad f_{\gamma,w} \propto (I_z)_w^{-1/2}$$

$$\frac{f_{v,a}}{f_{v,w}} = \sqrt{\frac{m}{m_a}}$$

But  $m_y = m_a + m_{\text{vir}}$  [E-5]

Therefore  $\frac{f_{v,a}^2}{f_{v,w}^2} = \frac{m + m_{\text{vir}}}{m_a} = 1 + \frac{m_{\text{vir}}}{m_a}$

---

\*In a fluid medium, this includes the virtual mass of the fluid as well as the structural mass; similarly for  $I_z$ .

Hence

$$m_{\text{vir}} = m_a \left[ \left( \frac{f_{v,a}}{f_{v,w}} \right)^2 - 1 \right] \quad [\text{E-6}]$$

This is Equation [18] of Table 1. An alternative method for computing  $M_{\text{vir}}$  based on Reference 15 is given by Equation [19] of Table 1.

Similarly, since

$$(I_z)_w = (I_z)_a + (I_z)_{\text{vir}}$$

assuming that  $M_{\text{vir}}$  and  $M_a$  lie close to the center of mass of the rudder in water (otherwise use the parallel axis theorem to transfer all moments to this latter center of mass; see footnote next page)

then

$$(I_z)_{\text{vir}} = (I_z)_a \left[ \left( \frac{f_{\gamma,a}}{f_{\gamma,w}} \right)^2 - 1 \right] \quad [\text{E-7}]$$

Finally, to treat  $\alpha$ - motions, we postulate

$$f_{\alpha,a} \propto (I_x)_a^{-1/2} \quad \text{and} \quad f_{\alpha,w} \propto (I_x)_w^{-1/2}$$

Then, making the same assumption as for  $(I_z)_w$ ,

$$(I_x)_w = (I_x)_a + (I_x)_{\text{vir}} \quad [\text{E-8}]$$

$$(I_x)_{\text{vir}} = (I_x)_a \left[ \left( \frac{f_{\alpha,a}}{f_{\alpha,w}} \right)^2 - 1 \right] \quad [\text{E-9}]$$

The methods for computing the frequencies of the coupled  $(v, \gamma)$  motions are given on pages 321 and 322 of Reference 9. The coordinates  $y$  and  $\gamma$  used here are  $x$  and  $\theta$ , respectively, in Reference 9.

Actually, for the ships under consideration, the frequencies that were used in calculating  $M_{\text{vir}}$ ,  $(I_z)_{\text{vir}}$  and  $(I_x)_{\text{vir}}$  are the predominant ones associated with measured coupled motions rather than the frequencies corresponding to the uncoupled motions. Thus since we cannot really discriminate between  $f_v$ ,  $f_\gamma$ , and  $f_\alpha$  in these calculations (if measured frequencies are used), Equations [E-6], [E-7], and [E-9] may lead to poor or questionable results. Calculation showed that use of Equation [E-6] for ALBACORE leads to satisfactory results whereas use of Equations [E-7] and [E-9] do not.\* Hence, alternative formulations for  $(I_z)_{\text{vir}}$  and  $(I_x)_{\text{vir}}$  based on Reference 15 are given by Equations [20] and [21], respectively, of Table 1. In Equations [20] and [21], note that the first terms in the right members are virtual mass moments of inertia of the rudder about a z- and a x-axis, respectively, through the center of mass; i. e., geometrical center of the ellipsoidal volume of water which approximates the volume of the rudder (see Reference 4 pages 11 and 12). The terms  $r^2 M_{\text{vir}}$  and  $s^2 M_{\text{vir}}$  transfer these moments to x- and y-axes through the center of mass of the entire rudder-fluid system; r and s are the distances between these x- and y-axes, respectively.

---

\*This follows from comparisons with the results of Equations [19], [20], and [21] of Table 1, respectively. In this case,  $f_v$  probably closely corresponds to the predominant frequency whereas  $f_\gamma$ ,  $f_\alpha$  do not. Hence, while the Equations [E-7] and [E-9] may be sound, the data inserted in them are of doubtful validity. In performing these calculations, all moments were transferred by means of the parallel axis theorem to axes with origin at the center of mass of the entire rudder-fluid system.

## REFERENCES

1. Kennard, E. H. and Leibowitz, R. C., "Theory of Rudder-Driving Plane-Ship Vibrations and Flutter, Including Methods of Solution," David Taylor Model Basin Report 1507 (Feb 1962).
2. Leibowitz, R. C. and Belz, D. J., "A Procedure for Computing the Hydroelastic Parameters for a Rudder in a Free Stream," David Taylor Model Basin Report 1508 (Apr 1962).
3. Leibowitz, R. C. and Belz, D. J., "Comparison of Theory and Experiment for Marine Control-Surface Flutter," David Taylor Model Basin Report 1567 (Aug 1962).
4. Leibowitz, R. C., "USS ALBACORE (AGSS 569) Modes of Rudder Vibration," David Taylor Model Basin Report 1540 (Sep 1961).
5. Leibowitz, R. C. and Kennard, E. H., "Theory of Freely Vibrating Nonuniform Beams Including Methods of Solution and Application to Ships," David Taylor Model Basin Report 1317 (May 1961).
6. Leibowitz, R. C. and Kennard, E. H., "Theoretical and Experimental Determination of Damping Constants of One-to-Three Dimensional Vibrating Systems," David Taylor Model Basin Report 1770 (Jun 1964).
7. Hoyt, Edgar D., "USS SAMPSON (DDG 10) Rudder Vibration Tests," Robert Taggart Inc. Technical Report prepared under contract NObs 86122 (4 Jan 1963).

8. McGoldrick, R. T., "Ship Vibration," David Taylor Model Basin Report 1451 (Dec 1960).
9. Bunyon, T. W., "A Study of the Cause of Some Rudder Failures," Northeast Coast Institution of Engineers and Shipbuilders, Vol. 68, Part 7 (May/June 1952).
10. Ayling, P. W. and Taylor, K. V., "Measurements of Strain and Vibration on the Rudder and Sternframe of a Single-screw Dry-cargo Ship of 13,000 SHP, Part I," The British Shipbuilding Research Association Report 383 (1962).
11. Mazet, R., "Some Aspects of Ground and Flight Vibration Tests," AGARD Report 40-T (Apr 1956).
12. Anderson, J. E. and Comley, W., "Transient Response Data Reduction and a Unique Transient Wave Analyzer," Proceedings of the AIEE Conference, Santa Monica, California (May 23-25, 1960).
13. Wolfe, M. O. W. and Kirkby, W. T., "Several Techniques for Flight Flutter Testing," Part I AGARDograph 56 (Sep 1960).
14. Stringham, R. H., Jr., "A Method for Measuring Vibration Modes of a Transiently Heated Structure," SAE-ASNE National Aeronautical Meeting, Washington, D. C. (8 Apr 1963).
15. Wendel, K., "Hydrodynamic Masses and Hydrodynamic Moments of Inertia" "(Hydrodynamische Massen and Hydrodynamische Massenträgheitsmomente)," Jahrb. d. STG, Volume 44 (1950). TMB Translation 260 (Jul 1956).





INITIAL DISTRIBUTION

Copies		Copies	
12	CHBUSHIPS	2	DIR, NASA
	3 Tech Lib (Code 210L)		1 Ship Struc Comm
	1 Lab Mgt (Code 320)	20	DDC
	1 Applied Res (Code 340)	1	WHOI
	1 Prelim Des Br (Code 420)	1	St. Anthony Falls Hydraul Lab
	1 Hull Des Br (Code 440)	5	MIT, Dept of (NAME)
	1 Sci & Res Sec (Code 442)	2	New York Univ
	1 Hull Struc Sec (Code 443)		1 Dept of Meteorology
	3 Ship Sil Br (Code 345)		1 Fluid Mech Lab
3	CHONR	1	Inst of Hydraul Res, Univ of Iowa
	1 Math Sci Div (Code 430)	1	Sch of Engin & Arch,
	1 Fluid Dyn Br (Code 438)		Catholic Univ
1	CHBUWEPS	2	Inst of Engin Res, Univ of
1	CO & DIR, USNMEL		California
1	CO & DIR, USNMDL	1	Head, Dept. of Nav Arch
1	CDR, USNOL		Attn: Prof Schade
1	CDR, USNOTS, China Lake	3	Univ of Michigan
1	CDR, USNOTS, Pasadena		1 Exper Naval Tank
1	DIR, USNRL		1 Dept of Engin Mech
1	CO, USNROTC & NAVADMINU MIT		1 Dir, Finn Michelson Dept of
1	Adm, Webb Inst.		Naval Arch
1	O in C, PGSCOL, Webb Inst.	1	Hudson Lab, Columbia Univ
1	NAVSHIPYD LBEACH (Code 240)	1	Univ of Notre Dame
1	NAVSHIPYD PEARL (Code 240)		Attn: Prof. A. Strandhagen,
1	NAVSHIPYD PUG (Code 240)		Head, Dept of Eng Mech
1	NAVSHIPYD SFRAN (Code 240)	1	APL, JHU
1	NAVSHIPYD NORVA (Code 240)	4	Fluid Dyn Res Grp, MIT
1	NAVSHIPYD PHILA (Code 240)		1 Mr. John Dugundsi
1	NAVSHIPYD BSN (Code 240)		1 Prof Holt Ashley
2	NAVSHIPYD NYK		1 Mrs. Sheila E. Widnall
	1 Des Supt (Code 240)		1 Mrs. Nancy Charles
1	USNASL	3	Dept of Applied Mech, SWRI
1	CMDT, USCG		1 Dr. H. Norman Abramson
	1 Secy, Ship Struc Comm		1 Mr. Wen-Hwa Chu
1	DIR, Natl BuStand		1 Mr. Jack T. Irick
1	ADM, MARAD	3	DIR, Davidson Lab, SIT
			1 Mr. Charles J. Henry
			1 Mr. Raihan Ali
		1	NNSB & DD Co.
			Attn: Mr. Montgomery

## Copies

1 Gen Dyn, EB Div

1 Polytechnic Inst of Bkly,  
Dept of Aerospace Eng &  
Applied Mechanics

2 SNAME  
1 Hull Struc Comm

4 Grumman Aircraft Eng Corp.  
1 Mr. Eugene F. Baird  
1 Mr. Charles E. Squires, Jr.  
1 Mr. Renso L. Caporali

2 Technical Research Group  
2 Aerial Way, Syosset, N.Y.  
1 Mr. Jack Kotik

1 Engineering Index, New York

1 Dr. E. H. Kennard  
4057 Tenago Road,  
Claremont, Calif

1 Dr. Theodore Theodorsen  
Republic Aircraft Corp,  
Farmingdale, L.I., N.Y.

1 Mr. I. E. Garrick, Langley  
Res Ctr, NASA,  
Langley Field, Va.

1 Mr. J. D. Crisp, Aeroelastic  
& Structures Res Lab, MIT

1 Mr. Maurice Sevik, College of  
Engin & Arch, ORL  
Penn State Univ

1 Mr. Alexander H. Flax, Cornell  
Aero Lab, Inc.

1 Mr. R. T. McGoldrick  
Box 293, Sheffield, Mass

1 MacNeal Schwendler Corp,  
2556 Mission Street  
San Marino, Calif

1 Prof M. Landahl, Dept of Aero  
and Astro, MIT,  
Cambridge 39, Mass

2 Hydronautics Inc, Pendell  
School Rd., Laurel, Md.

## Copies

2 President, Oceanics Inc,  
114 E 40 St., New York 16  
1 Mr. Paul Kaplan

1 J. G. Eng. Res. Associates  
3831 Menlo Dirve,  
Baltimore 15, Md.

3 Cornell Aeronautical Lab, Inc.  
Buffalo 21, New York  
1 Mr. Peter Crimi  
2 Mr. Irving C. Statler

3 General Dynamics, Convair  
P.O. Box 1950,  
San Diego 12, Cal  
1 Mr. Robert C. Peiler  
1 Mr. Louis M. Figueron

David Taylor Model Basin. Report 1836.  
EXPERIMENTAL DETERMINATION OF STRUCTURAL AND STILL  
WATER DAMPING AND VIRTUAL MASS OF CONTROL SURFACES,  
by Ralph C. Leibowitz and Arthur Kilcullen.  
Apr 1965, ix, 62p., illus., diagrs., refs.  
UNCLASSIFIED

An experiment has been designed for determining  
the damping constants and virtual mass for the con-  
trol surface systems of USS ALBACORE (AGSS 569) and  
USS SAMPSON (DDG 10); theoretical methods for  
determining the virtual inertias (including virtual  
mass) of these control surfaces are also given. The  
theoretical foundation for the experimental design  
and the procedure for analyzing the experimental  
data to obtain the parameters are described. These

1. Control surfaces--  
Vibration--Damping--  
Theory
2. Control surfaces--  
Vibration--Damping--  
Test results
3. Control surfaces--  
Virtual inertias--  
Theory
4. Control surfaces--  
Virtual inertias--  
Test results
5. Rudder-hull systems--  
Vibration--Damping--  
Theory

David Taylor Model Basin. Report 1836.  
EXPERIMENTAL DETERMINATION OF STRUCTURAL AND STILL  
WATER DAMPING AND VIRTUAL MASS OF CONTROL SURFACES,  
by Ralph C. Leibowitz and Arthur Kilcullen.  
Apr 1965, ix, 62p., illus., diagrs., refs.  
UNCLASSIFIED

An experiment has been designed for determining  
the damping constants and virtual mass for the con-  
trol surface systems of USS ALBACORE (AGSS 569) and  
USS SAMPSON (DDG 10); theoretical methods for  
determining the virtual inertias (including virtual  
mass) of these control surfaces are also given. The  
theoretical foundation for the experimental design  
and the procedure for analyzing the experimental  
data to obtain the parameters are described. These

1. Control surfaces--  
Vibration--Damping--  
Theory
2. Control surfaces--  
Vibration--Damping--  
Test results
3. Control surfaces--  
Virtual inertias--  
Theory
4. Control surfaces--  
Virtual inertias--  
Test results
5. Rudder-hull systems--  
Vibration--Damping--  
Theory

David Taylor Model Basin. Report 1836.  
EXPERIMENTAL DETERMINATION OF STRUCTURAL AND STILL  
WATER DAMPING AND VIRTUAL MASS OF CONTROL SURFACES,  
by Ralph C. Leibowitz and Arthur Kilcullen.  
Apr 1965, ix, 62p., illus., diagrs., refs.  
UNCLASSIFIED

An experiment has been designed for determining  
the damping constants and virtual mass for the con-  
trol surface systems of USS ALBACORE (AGSS 569) and  
USS SAMPSON (DDG 10); theoretical methods for  
determining the virtual inertias (including virtual  
mass) of these control surfaces are also given. The  
theoretical foundation for the experimental design  
and the procedure for analyzing the experimental  
data to obtain the parameters are described. These

1. Control surfaces--  
Vibration--Damping--  
Theory
2. Control surfaces--  
Vibration--Damping--  
Test results
3. Control surfaces--  
Virtual inertias--  
Theory
4. Control surfaces--  
Virtual inertias--  
Test results
5. Rudder-hull systems--  
Vibration--Damping--  
Theory

David Taylor Model Basin. Report 1836.  
EXPERIMENTAL DETERMINATION OF STRUCTURAL AND STILL  
WATER DAMPING AND VIRTUAL MASS OF CONTROL SURFACES,  
by Ralph C. Leibowitz and Arthur Kilcullen.  
Apr 1965, ix, 62p., illus., diagrs., refs.  
UNCLASSIFIED

An experiment has been designed for determining  
the damping constants and virtual mass for the con-  
trol surface systems of USS ALBACORE (AGSS 569) and  
USS SAMPSON (DDG 10); theoretical methods for  
determining the virtual inertias (including virtual  
mass) of these control surfaces are also given. The  
theoretical foundation for the experimental design  
and the procedure for analyzing the experimental  
data to obtain the parameters are described. These

1. Control surfaces--  
Vibration--Damping--  
Theory
2. Control surfaces--  
Vibration--Damping--  
Test results
3. Control surfaces--  
Virtual inertias--  
Theory
4. Control surfaces--  
Virtual inertias--  
Test results
5. Rudder-hull systems--  
Vibration--Damping--  
Theory

damping and inertial parameters are essential to the performance of a hull-control surface vibration and/or flutter analysis.

6. Rudder-hull systems--  
Vibration--Damping--  
Test Results
7. Experimental design
8. ALBACORE (U.S.  
auxiliary submarine,  
AGSS 569)
9. SAMPSON (U.S. guided  
missile destroyer  
DDG 10)
- I. Leibowitz, Ralph C.
- II. Kilcullen, Arthur

damping and inertial parameters are essential to the performance of a hull-control surface vibration and/or flutter analysis.

6. Rudder-hull systems--  
Vibration--Damping--  
Test Results
7. Experimental design
8. ALBACORE (U.S.  
auxiliary submarine,  
AGSS 569)
9. SAMPSON (U.S. guided  
missile destroyer  
DDG 10)
- I. Leibowitz, Ralph C.
- II. Kilcullen, Arthur

damping and inertial parameters are essential to the performance of a hull-control surface vibration and/or flutter analysis.

6. Rudder-hull systems--  
Vibration--Damping--  
Test Results
7. Experimental design
8. ALBACORE (U.S.  
auxiliary submarine,  
AGSS 569)
9. SAMPSON (U.S. guided  
missile destroyer  
DDG 10)
- I. Leibowitz, Ralph C.
- II. Kilcullen, Arthur

damping and inertial parameters are essential to the performance of a hull-control surface vibration and/or flutter analysis.

6. Rudder-hull systems--  
Vibration--Damping--  
Test Results
7. Experimental design
8. ALBACORE (U.S.  
auxiliary submarine,  
AGSS 569)
9. SAMPSON (U.S. guided  
missile destroyer  
DDG 10)
- I. Leibowitz, Ralph C.
- II. Kilcullen, Arthur

David Taylor Model Basin. Report 1836.  
EXPERIMENTAL DETERMINATION OF STRUCTURAL AND STILL  
WATER DAMPING AND VIRTUAL MASS OF CONTROL SURFACES,  
by Ralph C. Leibowitz and Arthur Kilcullen.  
Apr 1965, ix, 62p., illus., diagrs., refs.  
UNCLASSIFIED

An experiment has been designed for determining  
the damping constants and virtual mass for the con-  
trol surface systems of USS ALBACORE (AGSS 569) and  
USS SAMPSON (DDG 10); theoretical methods for  
determining the virtual inertias (including virtual  
mass) of these control surfaces are also given. The  
theoretical foundation for the experimental design  
and the procedure for analyzing the experimental  
data to obtain the parameters are described. These

1. Control surfaces--  
Vibration--Damping--  
Theory
2. Control surfaces--  
Vibration--Damping--  
Test results
3. Control surfaces--  
Virtual inertias--  
Theory
4. Control surfaces--  
Virtual inertias--  
Test results
5. Rudder-hull systems--  
Vibration--Damping--  
Theory

David Taylor Model Basin. Report 1836.  
EXPERIMENTAL DETERMINATION OF STRUCTURAL AND STILL  
WATER DAMPING AND VIRTUAL MASS OF CONTROL SURFACES,  
by Ralph C. Leibowitz and Arthur Kilcullen.  
Apr 1965, ix, 62p., illus., diagrs., refs.  
UNCLASSIFIED

An experiment has been designed for determining  
the damping constants and virtual mass for the con-  
trol surface systems of USS ALBACORE (AGSS 569) and  
USS SAMPSON (DDG 10); theoretical methods for  
determining the virtual inertias (including virtual  
mass) of these control surfaces are also given. The  
theoretical foundation for the experimental design  
and the procedure for analyzing the experimental  
data to obtain the parameters are described. These

1. Control surfaces--  
Vibration--Damping--  
Theory
2. Control surfaces--  
Vibration--Damping--  
Test results
3. Control surfaces--  
Virtual inertias--  
Theory
4. Control surfaces--  
Virtual inertias--  
Test results
5. Rudder-hull systems--  
Vibration--Damping--  
Theory

David Taylor Model Basin. Report 1836.  
EXPERIMENTAL DETERMINATION OF STRUCTURAL AND STILL  
WATER DAMPING AND VIRTUAL MASS OF CONTROL SURFACES,  
by Ralph C. Leibowitz and Arthur Kilcullen.  
Apr 1965, ix, 62p., illus., diagrs., refs.  
UNCLASSIFIED

An experiment has been designed for determining  
the damping constants and virtual mass for the con-  
trol surface systems of USS ALBACORE (AGSS 569) and  
USS SAMPSON (DDG 10); theoretical methods for  
determining the virtual inertias (including virtual  
mass) of these control surfaces are also given. The  
theoretical foundation for the experimental design  
and the procedure for analyzing the experimental  
data to obtain the parameters are described. These

1. Control surfaces--  
Vibration--Damping--  
Theory
2. Control surfaces--  
Vibration--Damping--  
Test results
3. Control surfaces--  
Virtual inertias--  
Theory
4. Control surfaces--  
Virtual inertias--  
Test results
5. Rudder-hull systems--  
Vibration--Damping--  
Theory

David Taylor Model Basin. Report 1836.  
EXPERIMENTAL DETERMINATION OF STRUCTURAL AND STILL  
WATER DAMPING AND VIRTUAL MASS OF CONTROL SURFACES,  
by Ralph C. Leibowitz and Arthur Kilcullen.  
Apr 1965, ix, 62p., illus., diagrs., refs.  
UNCLASSIFIED

An experiment has been designed for determining  
the damping constants and virtual mass for the con-  
trol surface systems of USS ALBACORE (AGSS 569) and  
USS SAMPSON (DDG 10); theoretical methods for  
determining the virtual inertias (including virtual  
mass) of these control surfaces are also given. The  
theoretical foundation for the experimental design  
and the procedure for analyzing the experimental  
data to obtain the parameters are described. These

1. Control surfaces--  
Vibration--Damping--  
Theory
2. Control surfaces--  
Vibration--Damping--  
Test results
3. Control surfaces--  
Virtual inertias--  
Theory
4. Control surfaces--  
Virtual inertias--  
Test results
5. Rudder-hull systems--  
Vibration--Damping--  
Theory

damping and inertial parameters are essential to the performance of a hull-control surface vibration and/or flutter analysis.

6. Rudder-hull systems--  
Vibration--Damping--  
Test Results
7. Experimental design
8. ALBACORE (U.S.  
auxiliary submarine,  
AGSS 569)
9. SAMPSON (U.S. guided  
missile destroyer  
DDG 10)
- I. Leibowitz, Ralph C.
- II. Kilcullen, Arthur

damping and inertial parameters are essential to the performance of a hull-control surface vibration and/or flutter analysis.

6. Rudder-hull systems--  
Vibration--Damping--  
Test Results
7. Experimental design
8. ALBACORE (U.S.  
auxiliary submarine,  
AGSS 569)
9. SAMPSON (U.S. guided  
missile destroyer  
DDG 10)
- I. Leibowitz, Ralph C.
- II. Kilcullen, Arthur

damping and inertial parameters are essential to the performance of a hull-control surface vibration and/or flutter analysis.

6. Rudder-hull systems--  
Vibration--Damping--  
Test Results
7. Experimental design
8. ALBACORE (U.S.  
auxiliary submarine,  
AGSS 569)
9. SAMPSON (U.S. guided  
missile destroyer  
DDG 10)
- I. Leibowitz, Ralph C.
- II. Kilcullen, Arthur

damping and inertial parameters are essential to the performance of a hull-control surface vibration and/or flutter analysis.

6. Rudder-hull systems--  
Vibration--Damping--  
Test Results
7. Experimental design
8. ALBACORE (U.S.  
auxiliary submarine,  
AGSS 569)
9. SAMPSON (U.S. guided  
missile destroyer  
DDG 10)
- I. Leibowitz, Ralph C.
- II. Kilcullen, Arthur

David Taylor Model Basin. Report 1836.  
EXPERIMENTAL DETERMINATION OF STRUCTURAL AND STILL  
WATER DAMPING AND VIRTUAL MASS OF CONTROL SURFACES,  
by Ralph C. Leibowitz and Arthur Kilcullen.  
Apr 1965, ix, 62p., illus., diagrs., refs.  
UNCLASSIFIED

An experiment has been designed for determining  
the damping constants and virtual mass for the con-  
trol surface systems of USS ALBACORE (AGSS 569) and  
USS SAMPSON (DDG 10); theoretical methods for  
determining the virtual inertias (including virtual  
mass) of these control surfaces are also given. The  
theoretical foundation for the experimental design  
and the procedure for analyzing the experimental  
data to obtain the parameters are described. These

1. Control surfaces--  
Vibration--Damping--  
Theory
2. Control surfaces--  
Vibration--Damping--  
Test results
3. Control surfaces--  
Virtual inertias--  
Theory
4. Control surfaces--  
Virtual inertias--  
Test results
5. Rudder-hull systems--  
Vibration--Damping--  
Theory

David Taylor Model Basin. Report 1836.  
EXPERIMENTAL DETERMINATION OF STRUCTURAL AND STILL  
WATER DAMPING AND VIRTUAL MASS OF CONTROL SURFACES,  
by Ralph C. Leibowitz and Arthur Kilcullen.  
Apr 1965, ix, 62p., illus., diagrs., refs.  
UNCLASSIFIED

An experiment has been designed for determining  
the damping constants and virtual mass for the con-  
trol surface systems of USS ALBACORE (AGSS 569) and  
USS SAMPSON (DDG 10); theoretical methods for  
determining the virtual inertias (including virtual  
mass) of these control surfaces are also given. The  
theoretical foundation for the experimental design  
and the procedure for analyzing the experimental  
data to obtain the parameters are described. These

1. Control surfaces--  
Vibration--Damping--  
Theory
2. Control surfaces--  
Vibration--Damping--  
Test results
3. Control surfaces--  
Virtual inertias--  
Theory
4. Control surfaces--  
Virtual inertias--  
Test results
5. Rudder-hull systems--  
Vibration--Damping--  
Theory

David Taylor Model Basin. Report 1836.  
EXPERIMENTAL DETERMINATION OF STRUCTURAL AND STILL  
WATER DAMPING AND VIRTUAL MASS OF CONTROL SURFACES,  
by Ralph C. Leibowitz and Arthur Kilcullen.  
Apr 1965, ix, 62p., illus., diagrs., refs.  
UNCLASSIFIED

An experiment has been designed for determining  
the damping constants and virtual mass for the con-  
trol surface systems of USS ALBACORE (AGSS 569) and  
USS SAMPSON (DDG 10); theoretical methods for  
determining the virtual inertias (including virtual  
mass) of these control surfaces are also given. The  
theoretical foundation for the experimental design  
and the procedure for analyzing the experimental  
data to obtain the parameters are described. These

1. Control surfaces--  
Vibration--Damping--  
Theory
2. Control surfaces--  
Vibration--Damping--  
Test results
3. Control surfaces--  
Virtual inertias--  
Theory
4. Control surfaces--  
Virtual inertias--  
Test results
5. Rudder-hull systems--  
Vibration--Damping--  
Theory

David Taylor Model Basin. Report 1836.  
EXPERIMENTAL DETERMINATION OF STRUCTURAL AND STILL  
WATER DAMPING AND VIRTUAL MASS OF CONTROL SURFACES,  
by Ralph C. Leibowitz and Arthur Kilcullen.  
Apr 1965, ix, 62p., illus., diagrs., refs.  
UNCLASSIFIED

An experiment has been designed for determining  
the damping constants and virtual mass for the con-  
trol surface systems of USS ALBACORE (AGSS 569) and  
USS SAMPSON (DDG 10); theoretical methods for  
determining the virtual inertias (including virtual  
mass) of these control surfaces are also given. The  
theoretical foundation for the experimental design  
and the procedure for analyzing the experimental  
data to obtain the parameters are described. These

1. Control surfaces--  
Vibration--Damping--  
Theory
2. Control surfaces--  
Vibration--Damping--  
Test results
3. Control surfaces--  
Virtual inertias--  
Theory
4. Control surfaces--  
Virtual inertias--  
Test results
5. Rudder-hull systems--  
Vibration--Damping--  
Theory

damping and inertial parameters are essential to the performance of a hull-control surface vibration and/or flutter analysis.

6. Rudder-hull systems--  
Vibration--Damping--  
Test Results
7. Experimental design
8. ALBACORE (U.S.  
auxiliary submarine,  
AGSS 569)
9. SAMPSON (U.S. guided  
missile destroyer  
DDG 10)
- I. Leibowitz, Ralph C.
- II. Kilcullen, Arthur

damping and inertial parameters are essential to the performance of a hull-control surface vibration and/or flutter analysis.

6. Rudder-hull systems--  
Vibration--Damping--  
Test Results
7. Experimental design
8. ALBACORE (U.S.  
auxiliary submarine,  
AGSS 569)
9. SAMPSON (U.S. guided  
missile destroyer  
DDG 10)
- I. Leibowitz, Ralph C.
- II. Kilcullen, Arthur

damping and inertial parameters are essential to the performance of a hull-control surface vibration and/or flutter analysis.

6. Rudder-hull systems--  
Vibration--Damping--  
Test Results
7. Experimental design
8. ALBACORE (U.S.  
auxiliary submarine,  
AGSS 569)
9. SAMPSON (U.S. guided  
missile destroyer  
DDG 10)
- I. Leibowitz, Ralph C.
- II. Kilcullen, Arthur

damping and inertial parameters are essential to the performance of a hull-control surface vibration and/or flutter analysis.

6. Rudder-hull systems--  
Vibration--Damping--  
Test Results
7. Experimental design
8. ALBACORE (U.S.  
auxiliary submarine,  
AGSS 569)
9. SAMPSON (U.S. guided  
missile destroyer  
DDG 10)
- I. Leibowitz, Ralph C.
- II. Kilcullen, Arthur



MIT LIBRARIES

DUPL



3 9080 02753 0242

